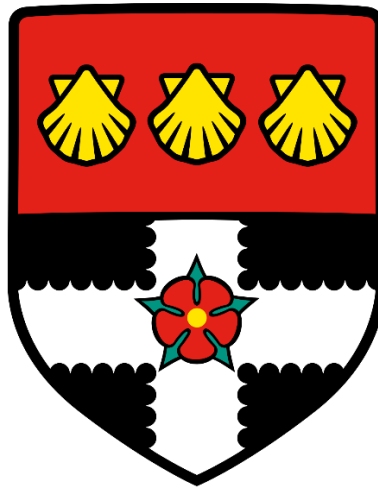


UNIVERSITY OF READING

Department of Meteorology



**Do the properties of convective clouds converge at
High-resolution?**

Walimunige Nadie Senali Rupasinghe

Personal email: nadierup@gmail.com

Supervisors: Dr. Robert Stephen Plant

Dr. Todd Jones

A dissertation submitted in partial fulfilment of the requirement for the degree of
MSc in Applied Meteorology and climate with management

8th August 2018

ACKNOWLEDGEMENT

First and foremost, I would like to express my sincere gratitude towards my supervisors Dr. R.S. Plant and Dr. T.R. Johns for their support and guidance throughout this period of dissertation. It was their interest on topic and timely comments led this project to be a success.

Secondly, I would like to thank World Meteorological organization, UK Met office and Department of Meteorology, Sri Lanka for granting me the financial support to fulfil the post graduate degree. Guidance and support provided by the director general and all the staff members of Department of Meteorology, Sri Lank are highly appreciated.

Further, I would like to thank my beloved parents, sister and all my friends for the moral support provided me throughout this year. Finally, my husband and parents-in-law for taking care of my daughter and letting me fulfil my dream. Thank you very much for believe in me!

ABSTRACT

Deep convection is a main source of precipitation on Earth. It also transports moist static energy to the upper troposphere, by interacting with the global circulation and by mass exchange between the troposphere and stratosphere, which is a main component in the balance of Earth's energy. Therefore, studying the properties of convection gains a lot of attention. Among various types of numerical models, "Convection permitting" numerical models are very useful in these studies as in-situ measurements of convective clouds using aircraft observations are very limited. These models run in the range of 1- 4 km resolution which simulate convective clouds explicitly without the need for a parameterization.

In this study, clouds were simulated at finer resolutions to determine cloud property variation. The aim is to investigate which resolution might determine cloud properties using the results produced by the new MONC (Met Office - NERC) cloud model, at resolutions 50, 100, 200, 400, 800, 1600 and 3200 m. Cloud properties and distributions of cloud properties based on simulated clouds were investigated to determine the best resolution which can be used with confidence.

Analysing the variation of cloud liquid water content and cloud fraction with height, 842 m level was selected as the vertical level for further analysis. Since the vertical wind velocity data has different height levels, data from 902 m and 785 m levels were averaged to study average vertical wind velocity distribution in clouds. Probability distribution functions of cloud liquid water content and vertical wind velocity behaved similarly for 3200, 1600 and 800 m resolutions and 200, 100 and 50 m resolutions also showed similar behaviour. 400 m had mixed behaviour of the two. Cloud identification algorithm was developed to extract cloud properties. Number of clouds larger than 1, 5, 10 and 20 km² decreased with increasing resolution while the number of clouds increased with resolution. Only 3200 m resolution has clouds larger than 10 km². There was not significant variation of average cloud liquid water content though there are higher number of clouds with small values in highest three resolutions. Cloud average vertical wind velocity distribution for 50 and 100 m resolutions were more symmetric with both updraft and downdrafts while the distributions became more asymmetric for lower resolutions and showed more updrafts. Based on the analysed data, 200, 100 and 50 m resolutions showed similar behaviours. Therefore, 200 m resolution can be used for further analysis with confidence.

ABBREVIATIONS

TTL	Tropical tropopause layer
GCMs	Global circulation models
CPMs	Convective permitting models
CRMs	Cloud – resolving models
LEMs	Large eddy models
MONC	Met Office - NERC
LWC, q_{cl}	Liquid water content
w	Vertical wind velocity
LCL	Lifting condensation level
RCE	Radiative – convective Equilibrium
SST	Sea surface temperature
OLR	Outgoing longwave radiation
ITCZ	Intertropical convergence zone
MCS	Mesoscale convective system
NWP	Numerical weather prediction
CAPE	Convective available potential energy
LES	Large eddy simulations
CSRM	Cloud system resolving model
JWCRP	Joint weather and climate research program
EPCC	Edinburgh Parallel Computing Centre
H_L	Latent heat
H_s	Sensible heat
PDF	Probability distribution function
GFDL	Geophysical fluid dynamic laboratory
HiCu	High-Plain cumulus
COPE	Convective precipitation experiment
ICE-T	Ice and clouds experiment - Tropical

TABLE OF CONTENTS

i.	Acknowledgement	
ii.	Abstract	
iii.	Abbreviation	
1.	Introduction	
1.1	Overview.....	1
1.2	Aim of the project.....	2
2.	Scientific Background	
2.1	Radiation energy budget.....	3
2.2	Radiative – Convective equilibrium.....	4
2.3	Cumulus clouds.....	5
2.4	Convective parameterization.....	8
2.5	“Convection permitting” models (CPMs).....	9
2.6	Large eddy models (LEMs).....	10
2.7	Sensitivity of the model.....	11
2.8	Cloud liquid water content (LWC, q_{cl})	11
2.9	Vertical wind velocity (w)	12
2.10	Distribution of cumulus cloud size.....	12
2.11	Liquid water flux.....	12
3.	Data and Methodology	
3.1	Met Office – NERC (MONC) model.....	13
3.2	Data description.....	13
3.3	Cloud counting algorithm and calculations.....	15
4.	Results and Discussion	
4.1	Determination of height level for the study.....	17
4.1.1	Variation of cloud liquid water content with height.....	17
4.1.2	Variation of cloud fraction with height.....	20
4.2	Statistical characteristics of convection.....	22

4.2.1	Cloud liquid water content.....	22
4.2.2	Vertical wind velocity.....	26
4.3	Cloud fraction variation with outputs.....	29
4.4	Cloud identification algorithm.....	30
4.5	Sensitivity of equilibrium convective ensemble statistics....	31
4.5.1	Distribution of cloud sizes.....	31
4.5.2	Average cloud liquid water content.....	41
4.5.3	Average vertical wind velocity.....	44
4.5.4	Distribution of cloud liquid water flux.....	48
5.	Conclusion and future work	
5.1	Summery.....	51
5.2	Conclusion.....	53
5.3	Future work.....	54
6.	References	55
7.	Appendix A	59

1. Introduction

1.1 Overview

Riehl and Malkus (1958) was the first paper published pointing out that moist convection plays major role in energy balance on Earth by transporting moist static energy to upper troposphere, by interacting with the global circulation and by mass exchange between troposphere and stratosphere. Tropical Tropopause Layer (TTL) water vapour budget may also have a major contribution from deep convection. (Liu and Zipser, 2005). Also, deep convection produces severe weather phenomenon like flash foods, cyclones, electrical storms and tornados which causes mass destructions to life (Stevens, 2005). Therefore, convection forecasting and further studies on cloud properties warrants attention.

Numerical models play main role in forecasting as well as further studies on weather phenomenon. They are very useful tool for a long time in studying convective cloud properties as it was difficult to carry out observational studies due to hazards of flight operations (in the presence, remote sensing data are used for observational studies) (Yang et al. 2016, Giangrande et al. 2016). On the other hand, these observations are not capable of obtaining observations at high spatial (100m) resolution. Global circulation models (GCMs), cloud permitting or cloud-resolving models (CPMs and CRMs) are widely used to study physical properties of convective clouds. GCMs are in the resolution range of 10s to 100s km while CPMs are in 1 – 4 km range. These models provide large amount of data points.

Large eddy models (LEMs) are very high-resolution models which can reach up to few meters of resolution used to study cloud properties. Met Office -NERC (MONC) model is a re – write of Met Office LEM. Data obtained from convective simulations from this model is used in this project.

1.2 Aim of the project

Main objective of this project was to investigate cloud properties and distributions of cloud properties based on simulated clouds to determine the best resolution which can be used with confidence. Cloud liquid water content (LWC, q_{cl}) and vertical wind velocity (w) data obtained from seven different resolutions of MONC model simulations were used for the study. Cloud distribution, cloud area and LWC and w properties were statistically analysed to determine the most suitable cost-effective resolution. Second objective was to develop a cloud identification algorithm to identify clouds in the field and extract cloud properties.

Rest of the report is organized as follow. Section 2 gives a brief description on the scientific background of the project. Then, description on MONC model and data analysis methodology are discussed in section 3. Next chapter discusses the results obtained during the analysis. Finally, conclusions and suggestions for future work are presented.

2. Scientific Background

2.1 Radiation energy budget

The fundamental energy source of Earth is the Sun. 29% of total energy received from sun is reflected due to albedo effect while the rest of it is absorbed by atmosphere (23%) and surface (48%). As seen in Figure 2.1, 5% of total absorbed energy leaves the surface through convection (NASA, 2009). Meteorological definition of convection is “small scale, thermally direct (usually vertical) circulations, driven by buoyancy (Emanuel 1994). When solar energy is absorbed by the surface (ocean and land), air near the surface become warmer than the higher altitudes. If this warmer unstable air is also moist enough, it become buoyant and form convective clouds upon reaching suitable height (Lifting condensation level, LCL). Convection also can occur due to cooling at the top of an air layer, lifting or saturation of a potentially unstable layer (Scheufele, 2014, Wageningen, 2010). Even though this process occurs both over land and ocean, land diurnal variation is more clearly visible. This process is more common in tropics as the highest amount of solar radiation is received in this region (Turner, 2018).

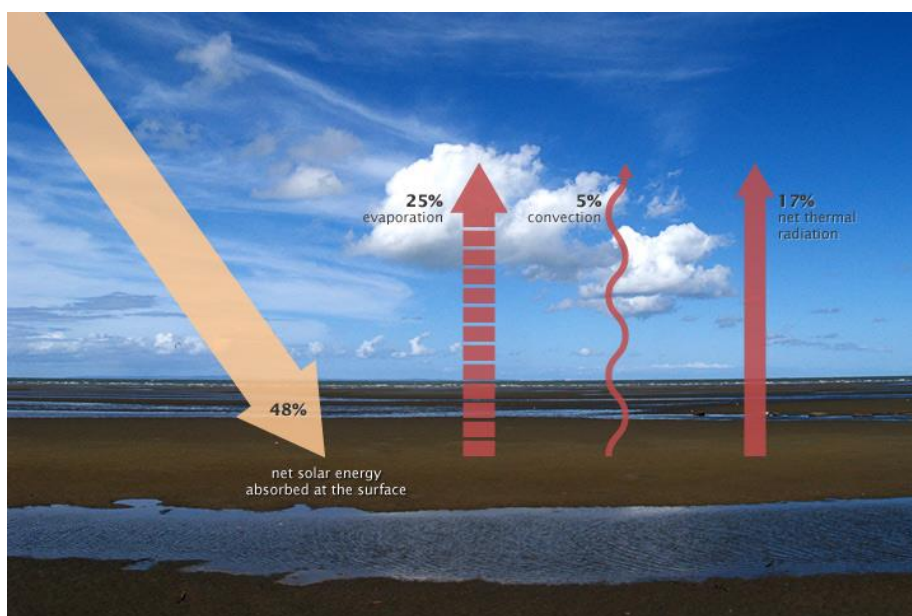


Figure 2.1: Schematic diagram of radiation energy budget (NASA, 2009).

Cumulus formation is favourable on days with clear mornings where the surface can heat up enough to make the low-level air unstable. It will then rise until it meets a stable layer such as inversion layer. Vertical distance between cloud base and condensation level (layer where temperature equals to the dew point) determines the formation of cumulus clouds. If the layer is stable enough, cloud tops are forced to develop horizontally (Wageningen, 2010). Also, for weak layers, cloud tops “shoot” through the layer and may continue to grow. Liu and Zipser (2005) found that 1.3% of tropical convection systems reach 14 km and 0.1% of them may penetrate the 380 K potential temperature level (the temperature that a sample of air attains if reduced to a pressure of 1000 millibars without receiving or losing heat to the environment). Further, they confirmed that this phenomenon is more common in land areas especially over central Africa, Indonesia and South America.

2.2 Radiative – Convective Equilibrium

According to Wing et al. (2017), Radiative – convective Equilibrium (RCE) is “the statistical equilibrium state that the atmosphere and surface would reach in the absence of lateral energy transport, in which there is a balance between net radiative cooling and convective heating”. This phenomenon was first introduced by Manabe and Wetherald in 1967. They have listed six main criteria for RCE at a given relative humidity as follow:

1. The net incoming solar radiation at the top of the atmosphere should be equal to the net outgoing long – wave radiation.
2. Temperature should be continuous.
3. The lapse rate should not exceed critical lapse rate of 6.5 C km^{-1} . This limit is maintained by free and forced convection and mixing by the large – scale eddies.
4. Conditions for RCE are fulfilled whenever the lapse rate is subcritical.
5. The Earth surface heat capacity is zero.
6. Given relative humidity is homogenous throughout the vertical profile of atmosphere (This assumption is no longer used in models).

Wing et al. 2017 state that these criteria with modifications were used in single – column models, two – and three- dimensional cloud – resolving models (section 2.5 and 2.6) and in regional/ global models (section 2.4) with convection parameterization to idealize the tropical weather. In most of the studies as well as in this study, an ocean is used as the surface boundary because interactions between vegetation, soil moisture and soil temperature create complications when land is used as the surface boundary (Rochetin et al., 2014).

2.3 Cumulus clouds

Riehl and Malkus (1958) first recognized that cumulus clouds transport moist static energy to upper troposphere, which is essential for global energy balance. Also, they are responsible for mass exchange between troposphere and stratosphere (Liu and Zipser, 2005; Scheufel 2014). As mentioned earlier in section 2.1, convection produces cumulus clouds which are the main generator of precipitation on Earth. They can be either stratocumulus clouds, shallow cumulus or deep precipitating cumulus (Stevens, 2005). Among these three types, last two are the most frequent types of convective clouds.

Stratocumulus clouds are low – level stratiform clouds originated mostly from breaking up of stratus clouds (Met Office, 2018, Stevens, 2005). Though these clouds only produce light drizzle, they are often misidentified as rain clouds and they exist in all types of weather. But they are mostly found in places where there is high thermal contrast between the overlying atmosphere and the underlying surface, for example, in upwelling regions of subtropical oceans and in storm tracks (Stevens, 2005).

Shallow cumulus convection is often seen in land during fair weather and occurs throughout the oceans (Stevens, 2005). The clouds are not tall enough for precipitation and therefore, “shallow” is used to describe these convective clouds. But shallow convection plays a main role in determining the vertical thermodynamic structure of atmosphere and affects the large-scale circulations in tropics as well as in subtropics. It is clearly visible in the Hadley cell over the ocean (Siebesma, 1998). It is responsible for exchanging sensible and latent heat between ocean and atmosphere, affecting earth’s surface, the top of the atmosphere radiation energy budget and the vertical momentum transport (Neggers et al. 2003).

Deep precipitation cumulonimbus clouds are formed by atmospheric moist convection. According to Stevens (2005), it is hypothesized that about 2000 non – diluting cumulonimbus

clouds with available area of 0.1 – 0.5 %, can fulfil the daily energy balance in the equatorial trough zone (low pressure zone). He also states that these clouds are favourable in oceans with sea surface temperatures (SST) warmer than 27-28 °C, surface wind converging zones and areas with high atmospheric relative humidity.

Figure 2.2 shows a schematic representation of physical processes in deep convective cumulus clouds. Conditionally unstable or unstable atmospheres are favourable for convection. Instability can have resulted from heating at the bottom of an air layer, cooling at the top of an air layer, lifting or saturation of an air layer or from a combination of all above. In this environment, unsaturated air parcel (warmer than environment) is stable for vertical displacement (Figure 2.2(1)). As air parcels ascend, they expand and cool so that at a certain height moisture will start condensing (weak OLR). At a certain height, air parcel become cool enough for condensation which gives extra energy source (latent heat) for air parcel to become unstable. At the same time, entrainment and turbulent mixing of environmental air occurs at edges (Figure 2.2(2)). When the air parcel is displaced to the level of neutral buoyancy, liquid water and cloud ice detrain at cloud top (Figure 2.2(3)) (Wageningen, 2010, Scheufele, 2014). Radiative cooling (1.5 to 2 K per day) occur in the dry clear descending parts atmosphere (Strong outgoing longwave radiation, OLR, Figure 2.2(4)) which is balanced by latent heat realised in precipitating deep convection clouds (eg: Intertropical convergence zone, ITCZ) (Mauritse and Stevens, 2015). Small water droplets collide each other and grow up until it is fall out as precipitation (Figure 2.2(5)). Downdrafts can occur due to the drag of air by the falling droplets and the formation of negative buoyancy due to cooling when precipitation re-evaporates into sub – saturated air, cooling when latent heat is supplied to melt ice at the freezing level (Figure 2.2(6)) (Turner, 2018).

Convection can often appear as an organized system spread through a wide space and time. When there is wind shear associated it can change the shape of the convective system. Importantly, it separates updraft and downdraft and the cold air from downdraft forces warm air to rise. This can lead to a very long-lived system and the system can propagate relative to the mean flow. There are three main types of convective systems namely, Squall lines, Mesoscale Convective Systems (MCS) and Superclusters (Turner, 2018).

There are three different ways of representing deep moist convection in numerical models. They are global models which simulate large-scale phenomena, cloud-resolving models and large – eddy models.

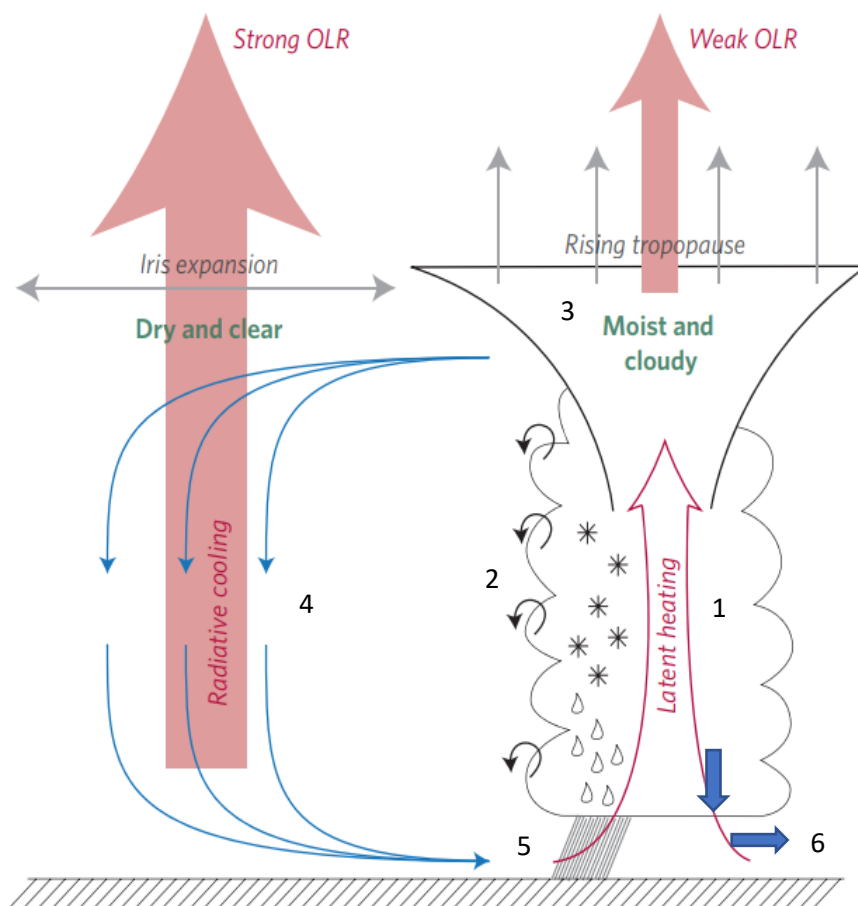


Figure 2.2: Schematic representation of tropical atmospheric circulation (Mauritse and Stevens, 2015) 1. Air parcel ascend. 2. entrainment and turbulent mixing of environmental air. 3. liquid water and cloud ice detrain at cloud top. 4. Radiative cooling occur in the dry clear descending parts atmosphere. 5. Formation of precipitation. 6. Downdrafts can occur due to the drag of air by the falling droplets.

2.4 Convective parameterization

Global circulation models (GCMs) simulating large – scale phenomena with a grid spacing in the order of 10 km need parameterization to represent convection in the model as the model cannot resolve cumulus clouds on the model grid. Typical cumulus clouds size is in the range of 1 – 2 km in diameter though the largest cloud diameters can extend up to around 10 km (Lennard 2004). Convection parameterization is based on the local-equilibrium hypothesis in which it is assumed that the unresolved convection within each grid box can only determine by large-scale resolved conditions (Scheufele, 2014). Convective parameterization must deal not only with heating rates due to transport and fluxes of sensible and latent heat but also with need to count the number of clouds which will then be able to feed into radiative scheme. Since convection acts as a major sink for atmospheric water vapour, determination of amount of precipitation also important (Inness, 2013).

A moist convective adjustment scheme was first introduced by Manabe et.al. in 1965 to introduce a simple convection scheme into models. This scheme distributed heating in the vertical direction so that an unstable profile moves towards the moist adiabat. In modern Numerical weather prediction (NWP) models, convective process usually treated as mass flux approach where the instability of vertical air column is considered through convective available potential energy (CAPE). At each level, heat and moisture will be changed either by detrainment of clouds into air or by entrainment of air from the outer environment. Temperature of the rising plume is calculated by the model and initiates condensation of water vapour. A similar method is used to adjust the cooling in downdraft due to cooling of precipitation falling through unsaturated parts of grid boxes (Inness, 2013).

Main problem with GCMs is that these models have a horizontal grid spacing around 200 km, which is not a good horizontal resolution appropriate for capturing individual clouds (Lennard 2004). Arakawa (2004) points out some other problems associated with cumulus parametrization. According to his review, main problem in conventional model physics is the uncertainties in the cloud formation processes since there is the absence of general framework to apply these processes. Further, conceptual problems are within the artificial separation of processes and of scales. The small scale direct interactions are missed out from the interactions between individual processes coursing through model's prognostic variables. The problem associated with the artificial separation of scales is due to the truncation of the atmospheric processes spectrum which is usually introduced for computational purposes. This

can influence the model by separating model physics into resolved and unresolved processes. Final main problem mentioned in Arakawa (2004) is the convergence in model physics. This is different from the problem arises in numerical analysis as the used equations for parameterization are modified or applied directly as possible not approximated. whereas it is not possible to apply known microphysical equations at this scale.

2.5 “Convection permitting” models (CPMs)

Convective permitting models or cloud – resolving models (CRMs) are Kilometre-scale models which can represent convection explicitly without the need for a parameterization scheme. In CPMs and CRMs, convective clouds can be represented on the grid scale, whereas in GCMs, they only exist via their parameterized influence, i.e., as subgrid features (Clark et al. 2016). In these models, large storms and mesoscale organization permitted but convective plumes and smaller showers are still not resolved. Orographic precipitation, convective storms and hourly rainfall characteristics, diurnal cycle of convection and urban and land-surface feedbacks can be forecasted with these high-resolution models (Fosser et al.). These models can produce qualitatively better precipitation fields thus better forecasts. They develop convection smoothly with better initiation time. Therefore, CPMs are useful in nowcasting (Charalambous, 2017).

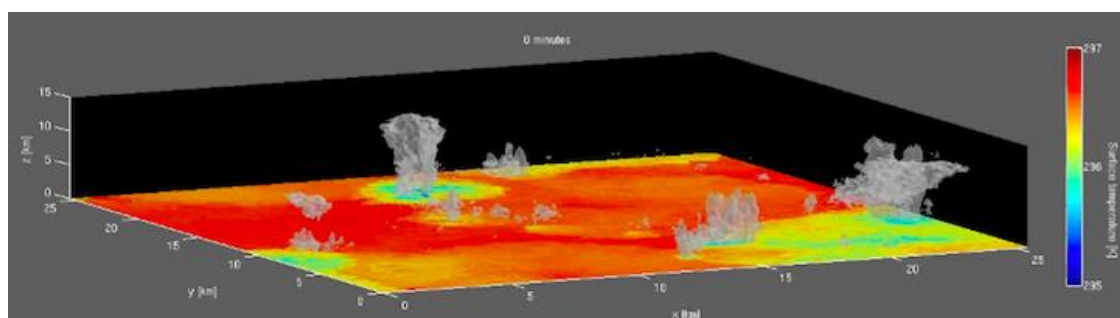


Figure 2.3: Snapshot of cloud-resolving simulation (Muller, C.).

CPMs let unstable convection to grow within the model. Latent heat released during condensation facilitates parts of the model to become buoyant compared to its surrounding so that vertical circulations can develop. These models usually contain a partial cloud cover parameterization which enables condensation when the resolved flow is still unsaturated. This cloud field consists of downdrafts, cloud-scale downdrafts and larger-scale subsidence. Each cloud has a life cycle which relate to other clouds letting cloud field to evolve through time. Sometime this leads to self-organization. Further, these models can produce positive feedbacks in precipitation formation and in deep convection through formation of cold pools from precipitation re-evaporation (Clark et al. 2016). Figure 2.3 shows a snapshot of a cloud-resolving model (colours indicate the surface temperature).

Even though CPMs are better than large-scale model, they also have disadvantages. These model's resolution ranging from 1 – 4 km are still not good enough to fully resolve individual convective elements. For example, Met Office's high-resolution UKV operational model tend to overestimate intense storms while underestimating number of small cell and do not predict enough light rains (Charalambous 2017).

2.6 Large eddy models (LEMs)

Large Eddy models (LEMs) have very fine grid spacings which allows individual cloud simulations through their full or over part of its life cycle. It is possible to simulate shallow cumulus, stratocumulus or storms and squall lines in the range of few meters to few kilometres in a 4D, time and space, domain of limited area using these models (Guichard and Couvreux 2017).

Both LEMs and CRMs can be used to study small, short lived shallow cumulus to wide, long lived deep convective clouds. The equations used in these models are also similar (non-hydrostatic types of models). But LEMs are designed to resolve turbulence motions to the inertial subrange because it is defined from the beginning. Main difference between these models are that the spatial resolution of CRMs is typically around 1 km which simulates deep convective clouds and for LEMs it is 100 m which also simulate shallow cumulus and stratocumulus (Guichard and Couvreux 2017, Gray 2003) (the highest resolution used in this study is 50 m as MONC model is rewrite of Met office LEM). Further, spatial grid spacing in large eddy simulations (LES) are usually close to isotropy ($dx = dy = dz = 50-100$ m) while in CRMs, it is stretched on the vertical with much finer discretization in the lower levels (< 100 m) and $dx = dy \sim 1$ km (highly anisotropic) (Guichard and Couvreux 2017). In this project, data

obtained from Met Office – NERC (MONC) LEM is used. Details of the model is discussed under section 3.1.

2.7 Sensitivity of the model

Sensitivity of a model data depends on the resolution of the model. However, high resolution requires high computational power. Therefore, it is important to determine the cost effective highest resolution which can capture important physical processes. This depends on the weather system investigated. For example, cloud system resolving model (CSRМ) with a horizontal resolution can be used to study behaviour of cloud system while 500 m or higher resolution should be needed to study propagation of a squall line (Pauluis and Garner 2006). Even though grid spacings of the order 1 km can capture basic structures of convective clouds, it is not good enough for further studies such as intracloud motions and sub-cloud scale turbulent eddies (Scheufele, 2014). Therefore, it is important to identify the cloud-resolving resolution which can be used to study convective clouds with confident. In this study, cloud liquid water content and vertical wind velocity data were used to investigate the sensitivity of MONC model.

2.8 Cloud liquid water content (LWC, q_{cl})

Microphysical and dynamical processes of clouds are directly connected with the LWC of the cloud (Devasthale and Thomas, 2012). It is different from cloud to cloud. Convective clouds show the highest amount of LWC and it is increasing with height up to the level of glaciation. LWC also increases with the cloud base height of the convective cloud. There are five different zones of LWC within a deep convective cloud namely from top to bottom of the cloud, glaciation, ice and droplet mixture, ‘rainout’ layer, zone of rapid droplet growth by coalescence of droplets above 0 °C and bottom most zone of very slow growth by diffusion (University of Wyoming).

Calheiros and Machado (2014) states that the quantity of water in a cloud affects the amount of latent heat, the updraft and downdraft within the cloud and the energy balance within the cloud. LWC in a convective cloud varies initially from approximately 0.2 g m^{-3} to 14 g m^{-3} during severe storm (Pruppacher and Klett, 1997). Given the range of possible liquid cloud characteristics in nature, it is interested in determining the extent to which MONC model can capture them as horizontal resolution is changed.

2.9 Vertical wind velocity (w)

Vertical wind velocity data obtained from the MONC model also used to study the sensitivity of the model. Vertical transport of cloud condensate, cloud top height, the detrainment into anvil, aerosol activation, droplet condensation, ice nucleation in convective clouds, precipitation efficiency and cloud life cycle are determined by the vertical wind velocity (Yang et al. 2016). Complexity of vertical velocity structure makes difficulties when it is parameterized. On the other hand, vertical velocity observations were limited due to hazards of flight operations in deep convective clouds. Therefore, high resolution simulation models are more suitable for studying this property (Yang et al. 2016, Giangrande et al. 2016).

2.10 Distribution of cumulus cloud size

Plank, 1969 was one of the first studies carried out to study cloud sizes. He investigated clouds photographed over Florida and observed that the number density of the cumulus clouds has an approximately exponential decrease with increasing cloud diameter in the early mornings. But, his theory did not support the cloud distribution in afternoons. After that various observational studies were carried out to determine the cloud area distribution (Scheufele, 2014, Lennard, 2004). They suggested log – normal, single power law or double power law distributions (Lopez, 1977, Machado and Rossow, 1993, Cahalan and Joseph, 1989).

In this study, statistical analysis of cloud area has been performed. But the focus is on any changes with model resolution rather than finding a formula to fit the area distribution. Data were extracted using cloud identification algorithm and were compared with each resolution

2.11 Cloud liquid water flux

Not like cloud area, cloud liquid water flux cannot be determined by observations. Therefore, numerical simulations studies are important in determining the liquid water flux variations within clouds. This indicates the liquid water transport within the cloud. Updraft and downdraft determines whether water is carried upwards or downwards.

3. Data and Methodology

3.1 Met Office – NERC (MONC) Model

MONC model is a highly scalable LES model (section 2.6) that has been developed to simulate clouds and turbulent flows at high resolution (~ 10 s to 100 s of metres meters) on large domains. Met Office LEM was used since the 1980s as a principal modelling tool to study atmospheric flows, turbulence and cloud microphysics. It included an operational radiative transfer scheme and a detailed cloud microphysics representation (Brown et al. 2015). The main limitations of this model were that the build process and code management method were archaic and the code structure limited domain size and length of stimulations. Therefore, the MONC project was initially funded through the Joint Weather and Climate Research Program (JWCRP), which facilitated collaboration between Met Office scientists and computational scientists at Edinburgh Parallel Computing Centre (EPCC). MONC model is a rewrite of Met Office LEM which enables the scientific community to work in further high resolution and on large space and time scale.

3.2 Data description

Cloud liquid water content (qcl) and vertical wind velocity (w) data obtained from convective cloud stimulations for seven different resolutions from the MONC model were used in this project (Table 3.1). Smaller domain sizes were used for higher resolutions as it takes more computational power and runtime.

Figure 3.1 shows an example of RCE simulation transition from the initial state to an equilibrated state (for 200 m resolution). Other resolutions were also proceeded in a similar manner with prescribe cooling of 1.5 K day^{-1} . The model top is at 40 km with surface pressure at 1000 hPa and SST at 300 K. Constant initial horizontal wind profiles are specified ($u = 5 \text{ ms}^{-1}$; $v = 0 \text{ ms}^{-1}$), and they are relaxed to these values with a timescale of 6 hours. The time steps have irregular spacing since model chooses time steps according to the importance of the processes going through the run. Therefore, the output time spacing is smaller if the process gives more data.

Table 3.1: Description of data used for analysis

Resolution / m	Domain size dx =dy / km	Diagnostic record length / days	Number of grid points	Number of outputs q_{cl} and w each
3200	134.4	42.5	42 × 42	27
1600	134.4	44	84 × 84	27
800	132.8	38.8	166 × 166	27
400	132.0	42.75	330 × 330	27
200	132.0	42.25	1320 × 1320	19
100	132.0	5.6	1320 × 1320	19
50	66.0	6.6	1320 × 1320	19

* The data was sampled in time such that each point in time can be considered independent.

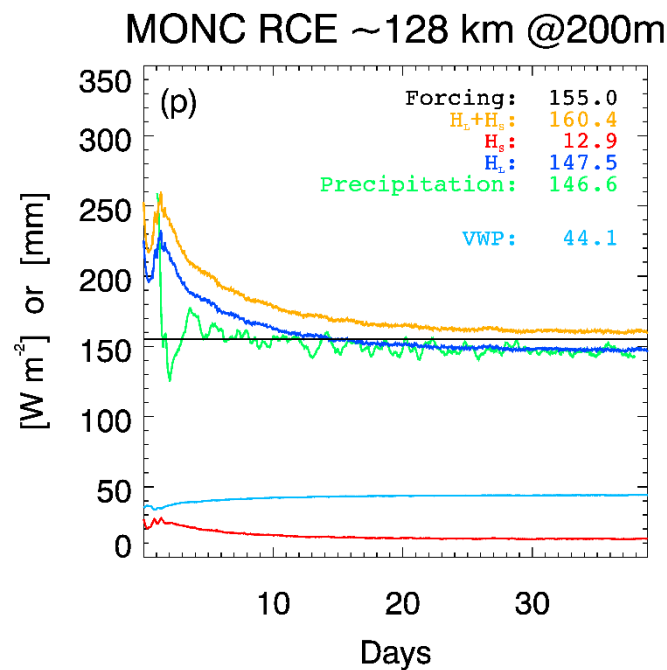


Figure 3.1: For 200 m resolution: The time series of domain mean integrated forcing (prescribed cooling), latent, H_L , and sensible, H_S , heat fluxes, precipitation rate (all in units of $W m^{-2}$), and integrated water vapor path (mm). Values are an average over days 30-40 (courtesy: Dr. T. Jones).

3.3 Cloud identification algorithm and calculations

First, the variation of average cloud liquid water content (q_{cl}) for each resolution with height were plotted to determine a suitable height level for further analysis. This was confirmed by a similar graph plotted with cloud fraction, where cloud points were determined at the points where q_{cl} is greater than 1×10^{-6} kg/kg. Depending on these results, 842 m height level was used for further analysis. Probability distribution functions (PDF) for q_{cl} and w were plotted to investigate the reproducibility of data at coarse resolutions.

Cloud identification algorithm was developed using Python computer programming language to determine the number of clouds, cloud size, and centre of clouds. The algorithm works as follow. First, q_{cl} data were loaded up into the Python program in the form of NetCDF files, and 842 m height level data was obtained. Then, data were converted into a binary array by considering points where q_{cl} is greater than 1×10^{-6} kg/kg is 1 and rest are 0. Cloud structures were identified using $[[1,1,1], [1,1,1], [1,1,1]]$ structure where if the algorithm recognize another cloud point adjacent to one of a cloud point then both points are recognized as one cloud (Figure 3.2). After that, first column and last column, as well as first row and last row were rechecked for connecting clouds at the ends as axis are connected by rollover. Figure 3.3 shows an example for such a situation. Blue squares indicate the points where there are edge clouds on same or neighbouring indexes which should be considered as parts of one single cloud. Labels were relabelled if connecting clouds are present in the edges. Finally, the number of clouds, cloud size, and centre of clouds were determined using the labels. These data were used to analyse the variation of average q_{clc} , w_c and mass flux ($q_{clc} \times w_c$) in clouds, the variation of cloud sizes and the number of clouds with resolution.

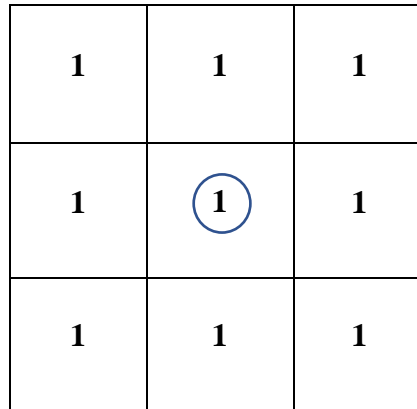


Figure 3.2: Structure of cloud identification algorithm. If algorithm identify cloud at middle (blue circle), it will check all neighbouring 8 positions for another object. If there exist any object both will be identified as one object and give the same label.

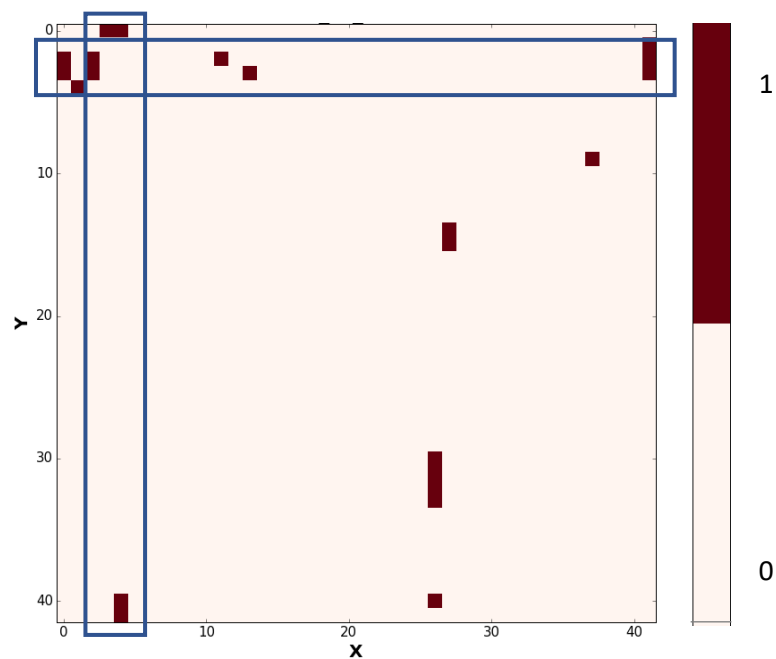


Figure 3.3: Snapshot of cloud distribution at 842 m level in 3200 m resolution (Cloud fraction = 0.01247).

4. Results and Discussion

This chapter discusses the results obtained during the dissertation. First step of the analysis was to determine a height level to carry out the further analysis. Cloud LWC and cloud fraction were investigated to determine vertical level where most of the clouds can be identified so that more data available for further analysis on cloud properties. After the deciding a vertical level, probability distributions functions of LWC and vertical wind velocity were analysed. This was performed for the whole data set within the vertical level to determine whether data are reproducible at coarse resolutions. Further, cloud fraction variation for each timestep in each resolution was plotted to have an idea about the data simulation variability of the model.

Next, cloud identification algorithm was developed to identify clouds and extract cloud properties, number of clouds, area of clouds, average LWC and average vertical wind velocity. These data distributions were further analysed to determine a suitable resolution at which cloud properties converge.

4.1 Determination of height level for the study

First step of analysis was to determine a suitable height level for further analysis. Therefore, variation of q_{cl} and cloud fraction with height was investigated. Results obtained were compared with the published data to determine a suitable height with largest amount of clouds.

4.3.1 Variation of cloud liquid water content with height

Therefore, q_{cl} was averaged over each time step in each resolution. Figure 4.1 shows the comparison of average q_{cl} for each resolution. It is clearly seen in the figure that higher the resolution, higher the average q_{cl} where the highest q_{cl} for 3200 m resolution is 0.3×10^{-5} kg/kg at 1752 m while 0.9×10^{-5} kg/kg for 50 m resolution at 1095 m. Further, 3200 m and 1600 m resolutions exhibit similar value variation.

Calheiros and Machado (2014) studied the LWC variation with height using remote sensing data (polarimetric variables from dual polarization radar) observed at four different sites in Brazil (Figure 4.2 (a)). This graph shows a similar variation as the simulated data from

MONC model and the highest amount of q_{cl} was observed around 500 - 1000 m. Similar study carried out by Iltoviz and Khain (2016) using Hebrew university cloud model also shows comparable behaviour of LWC (Figure 4.2 (b)) to the data obtained in MONC model.

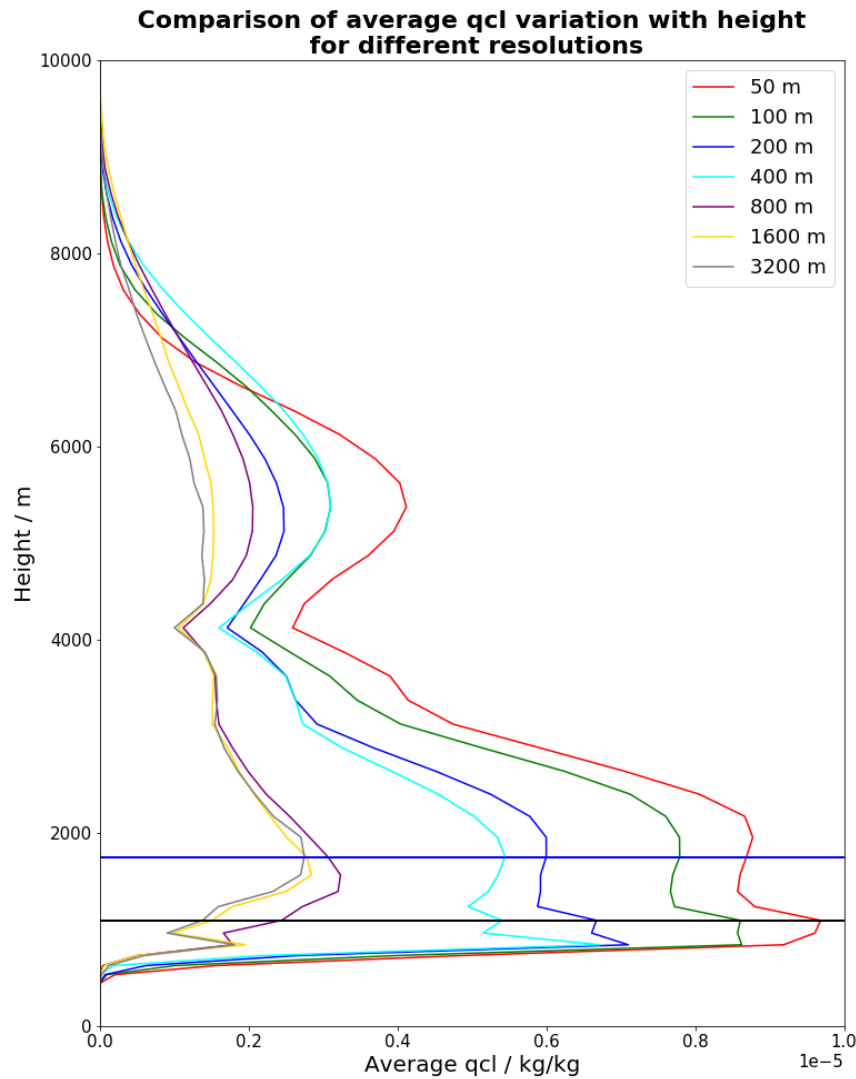


Figure 4.1: Variation of average q_{cl} with height. Black line: Highest q_{cl} height level for high resolution data (1095 m). Blue line: Highest q_{cl} height level for low resolution data (1752 m).

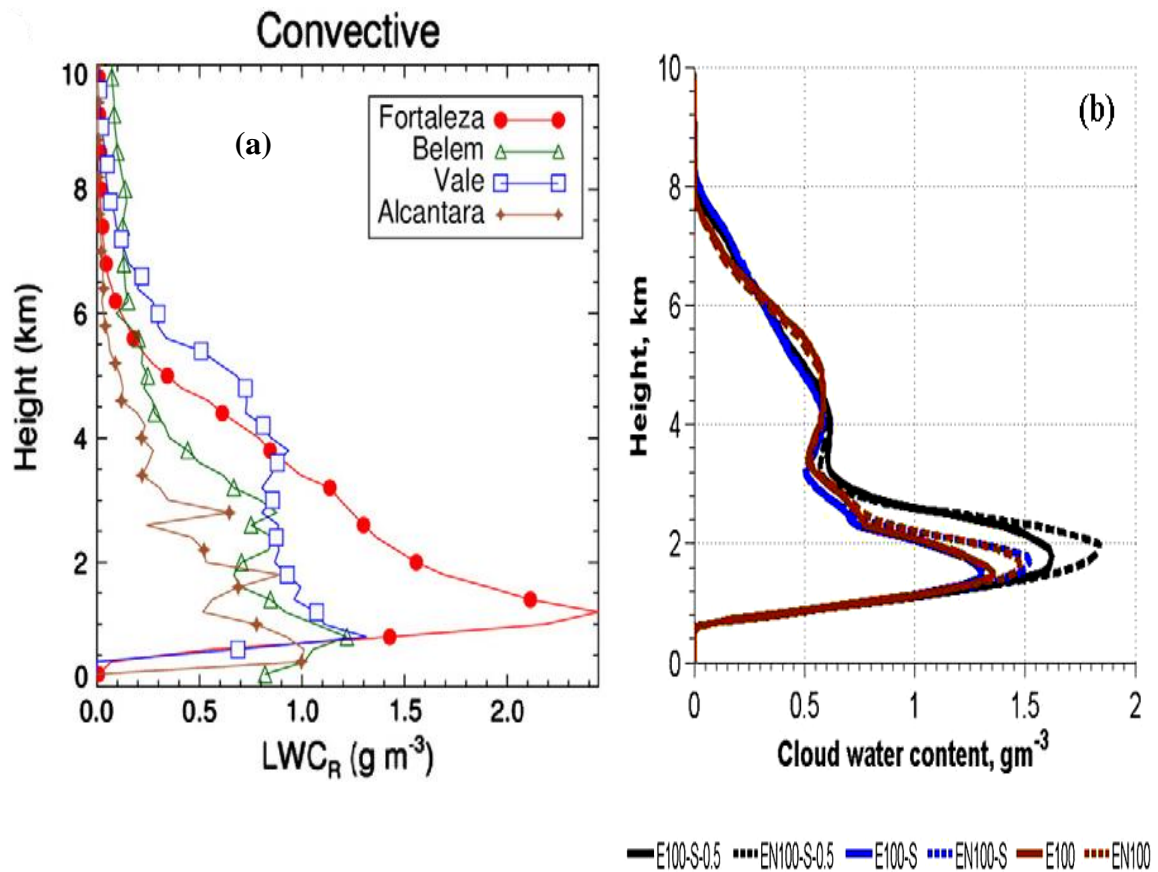


Figure 4.2: (a) Variation of LWC with height observed in four sites in Brazil (Fortaleza, Belem, Vale and Alcantara) by Calheiros and Machado (2014). (b) Variation of LWC with height simulated using Hebrew University Cloud Model (HUCM) with spectral (bin) microphysics by Iltoviz and Khain (2016).

4.3.2 Variation of cloud fraction with height

Since different resolution showed different heights with maximum average q_{cl} , average cloud fraction was calculated and its variation with height was plotted. LWC greater than 1×10^{-6} kg/kg were considered as points where clouds are present. According to Figure 4.3, most of the resolutions have maximum cloud fraction at 842 m.

In Figure 4.3, lowest two resolutions show similar variation with the maximum cloud fraction of 1.25 % for 3200 m and 1.5 % for 1600 m. When the resolution becomes higher, the cloud fraction also increases. It is 4.5 % for the highest resolution of 50 m. Therefore, it is clear from both Figures 4.1 and 4.3 that higher the resolution, more LWC data are captured.

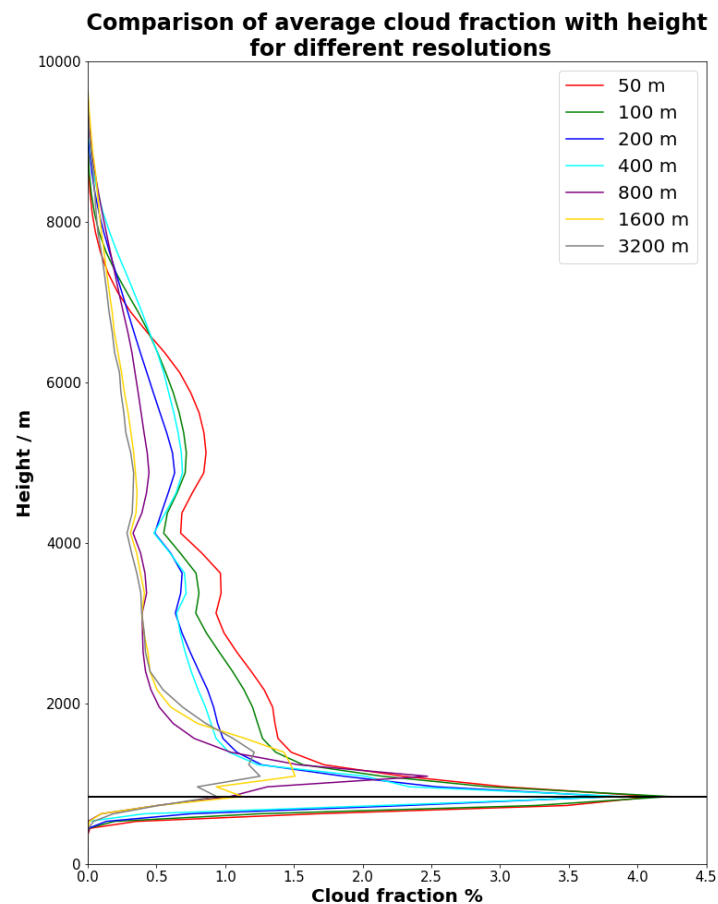


Figure 4.3: Cloud fraction variation with height. Black line: Highest q_{cl} height level for high resolution data (842 m).

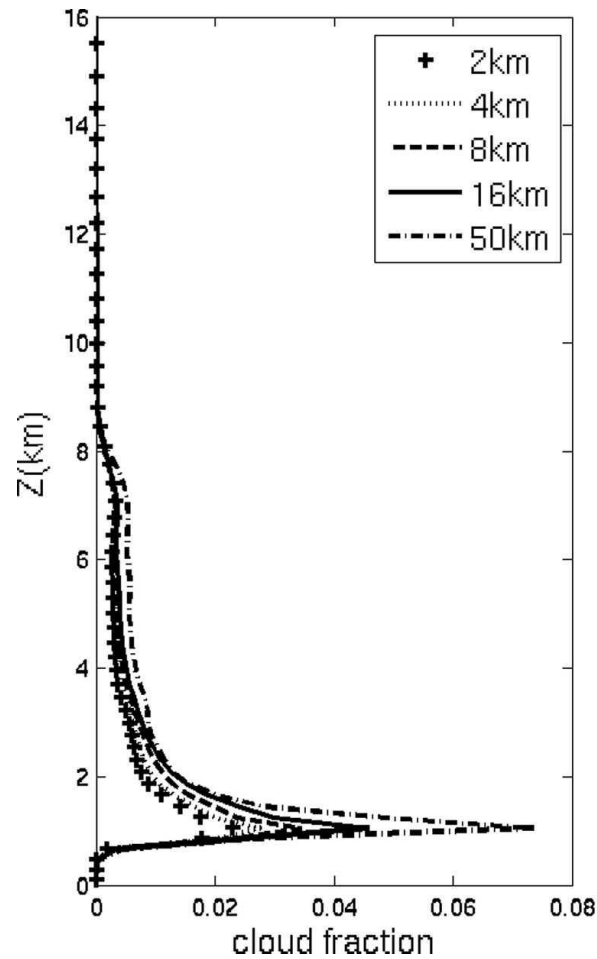


Figure 4.4: variation of cloud fraction with height (a) Pauluis and Garner, 2006.

Figure 4.4(a) shows the results published by Pauluis and Garner (2006) on their study carried out to determine the sensitivity of Geophysical Fluid Dynamic Laboratory (GFDL) climate model horizontal resolution (2, 4, 8, 16, 50 km resolutions) in RCE simulations. Resolutions were ranged from 50 – 2 km. As seen in the figure, not like in this project, lowest resolution shows the highest cloud fraction. But the height level and the variation are similar to this study. Depending on the results obtained for average qcl and cloud fraction and by comparing them with the literature, 842 m was selected as the height level for further analysis.

4.2 Statistical characteristics of convection

It is important to obtain a statistical description of convection system because it provides information of whether the coarse resolution can reproduce probability distribution functions (PDF) obtained at high resolutions (Pauluis and Garner, 2006). LWC and vertical wind velocity PDF are investigated in this study.

4.2.1 Cloud liquid water content

Figures 4.5, 4.6 and 4.7 shows cloud LWC PDF for each resolution at 842 m height level. Data are normalized so that the summation of all data gives 1. Here smaller LWC points indicates cloud free areas. As seen in Figure 4.5, lowest four resolutions have less cloud free areas compared to highest four resolutions. Further, highest three resolution captured more cloudy areas compared to lower four resolutions. 400 m resolution showed combination of two distribution behaviours. It exhibits high cloud free areas in line with 200, 100 and 50 m resolutions while low cloud free areas comparable with lowest three resolutions. Histograms shown in Figure 4.6 and 4.7 illustrates the distribution of q_{cl} in each resolution. Even though, most of the data lying within the 0 to 0.4×10^{-3} kg/kg range (more cloud free areas), number of cloudy areas is increasing with the resolution. Since there is no significant change in PDF at high resolutions (Figure 4.7), the model capable of reproducing q_{cl} data at high resolution.

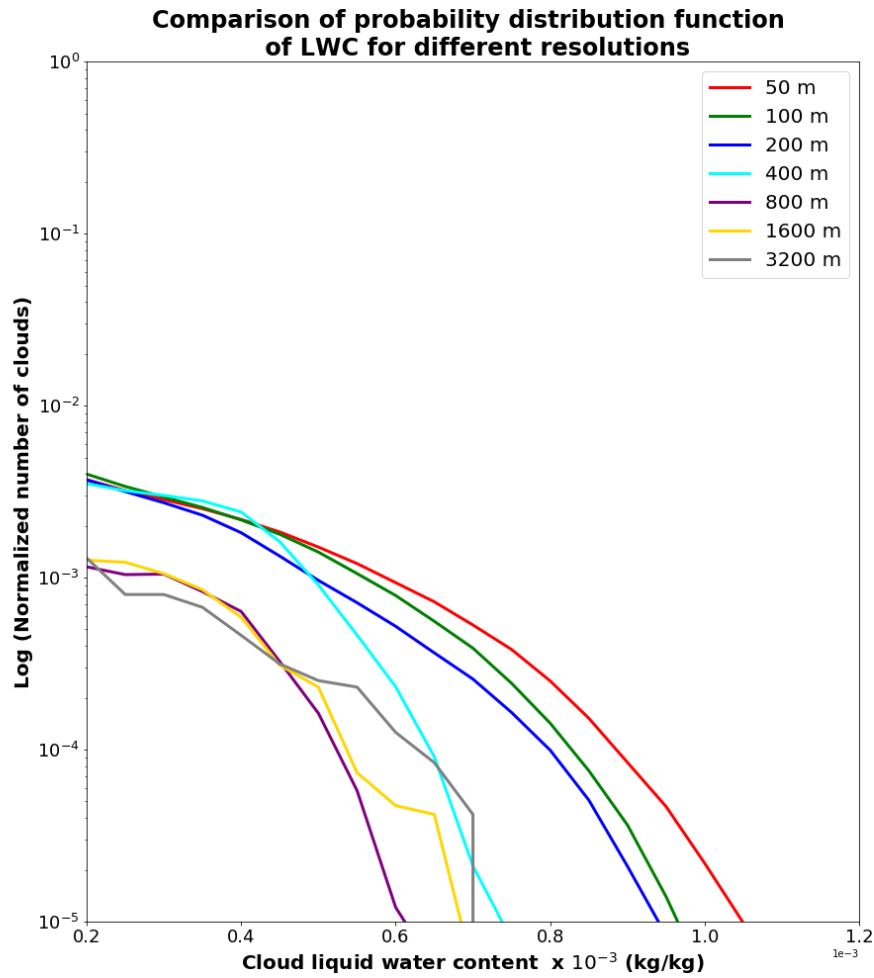


Figure 4.5: Probability distribution function comparison of LWC for 3200 (grey), 1600 (yellow), 800(purple), 400 (light blue), 200 (blue), 100 (green), 50 (red) m resolutions in normalized log – scale. The normalization was done so that the sum of all data to be 1.

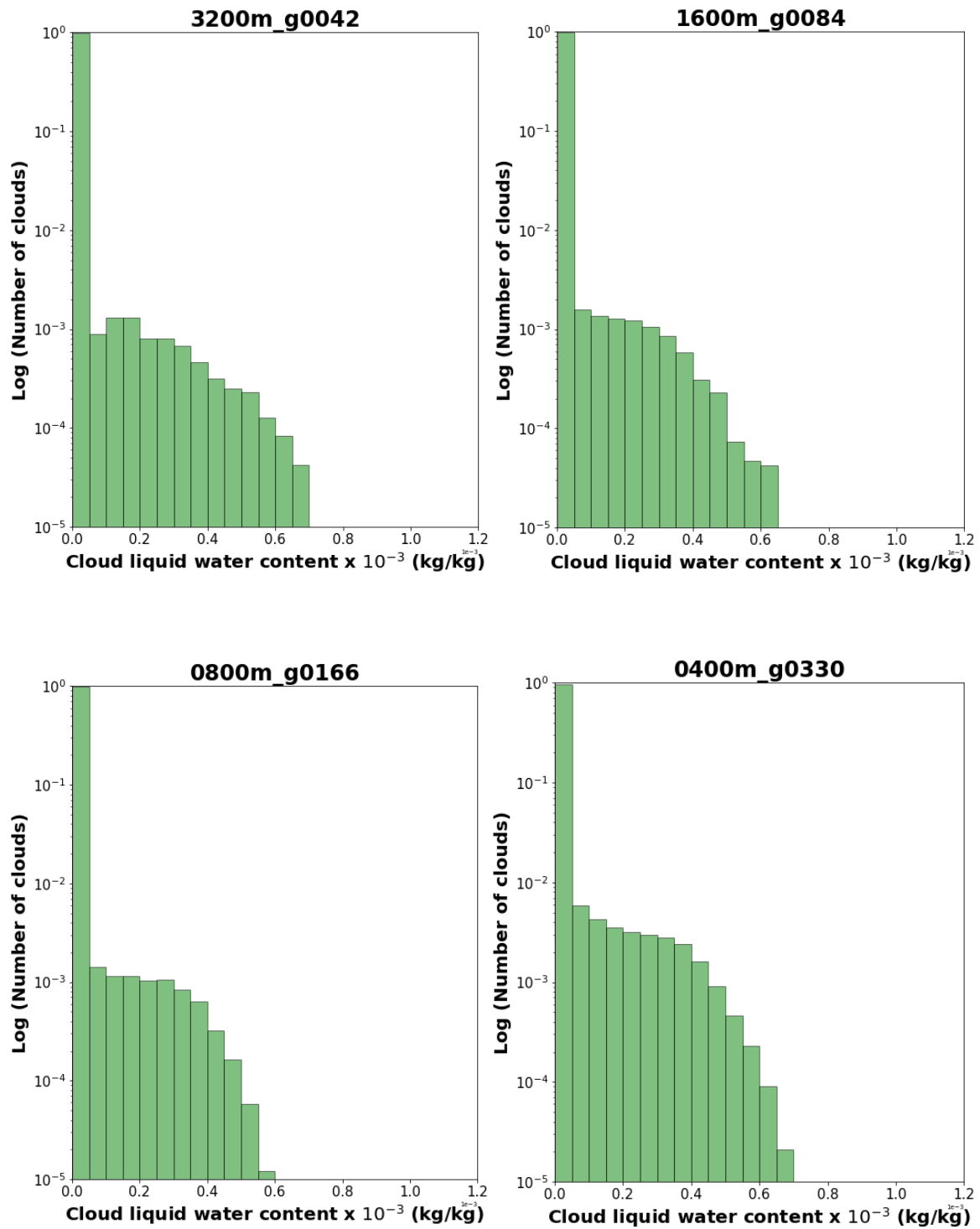


Figure 4.6: Distribution of cloud LWC data for 3200, 1600, 800 and 400 m resolutions in normalized log – space.

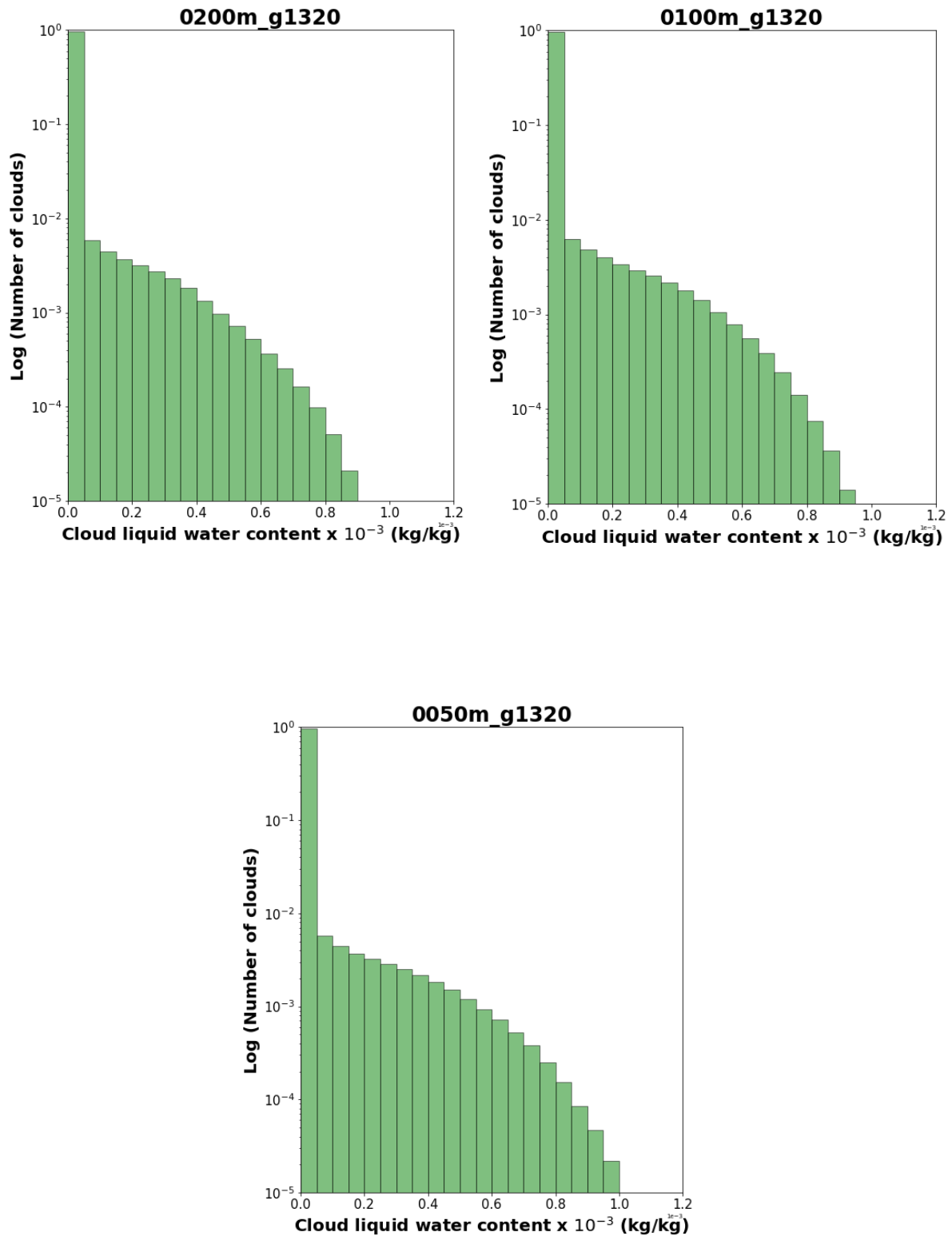


Figure 4.7: Distribution of cloud LWC data for 200, 100 and 50 m resolutions in normalized log – space.

4.2.2 Vertical wind velocity

Next, vertical wind velocity data were statistically investigated. Figures 4.8, 4.9 and 4.10 shows the data distribution of w data obtained from the MONC model at 901 m height level. Data were normalized so that the summation of all points gives 1. Here, positive values indicate the updraft while negative values indicate downdrafts. As seen in Figure 4.8, lowest resolution has more symmetric distribution while when resolution is increased, distribution becomes more asymmetric. It tends to capture more updraft data compared to downdraft. Pauluis and Garner, 2006 showed similar trend in their study carried out for resolutions 2 - 50 km. Same as in their study, the vertical velocity at highest resolution is about double the value of lowest resolution (Figure 4.9 and 4.10). In this distribution, the lowest three resolutions exhibits similar behaviour while highest three are similar. 400 m resolution shows similar behaviour with high resolutions for downdrafts while similar behaviour with low resolutions for updrafts for data more than 3 ms^{-1} .

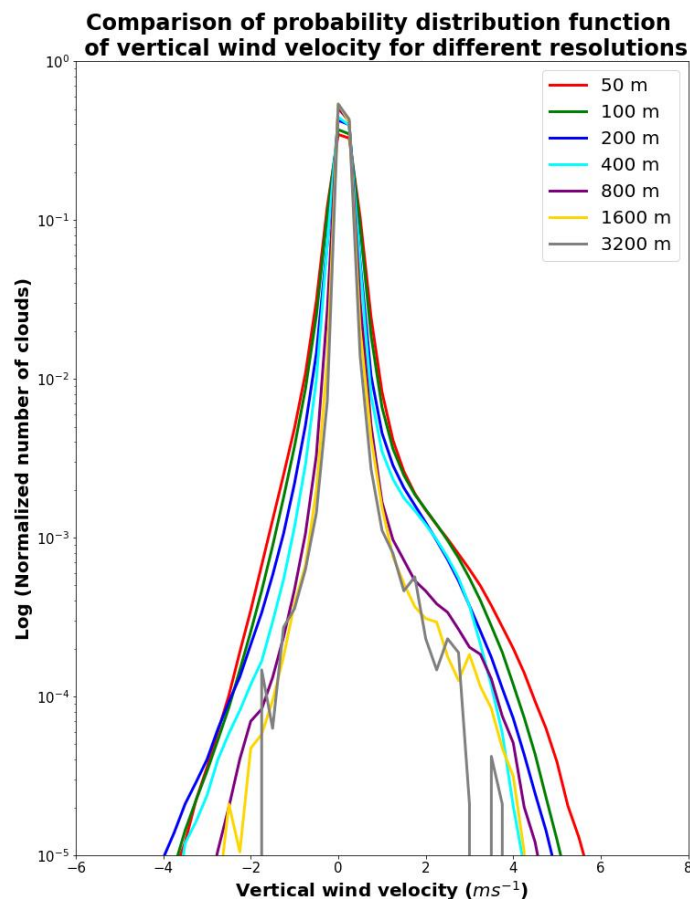


Figure 4.8: Probability distribution function comparison of vertical wind velocity for 3200 (grey), 1600 (yellow), 800 (purple), 400 (light blue), 200 (blue), 100 (green), 50 (red) m resolutions in normalized log – scale. The normalization was done so that the sum of all data to be 1.

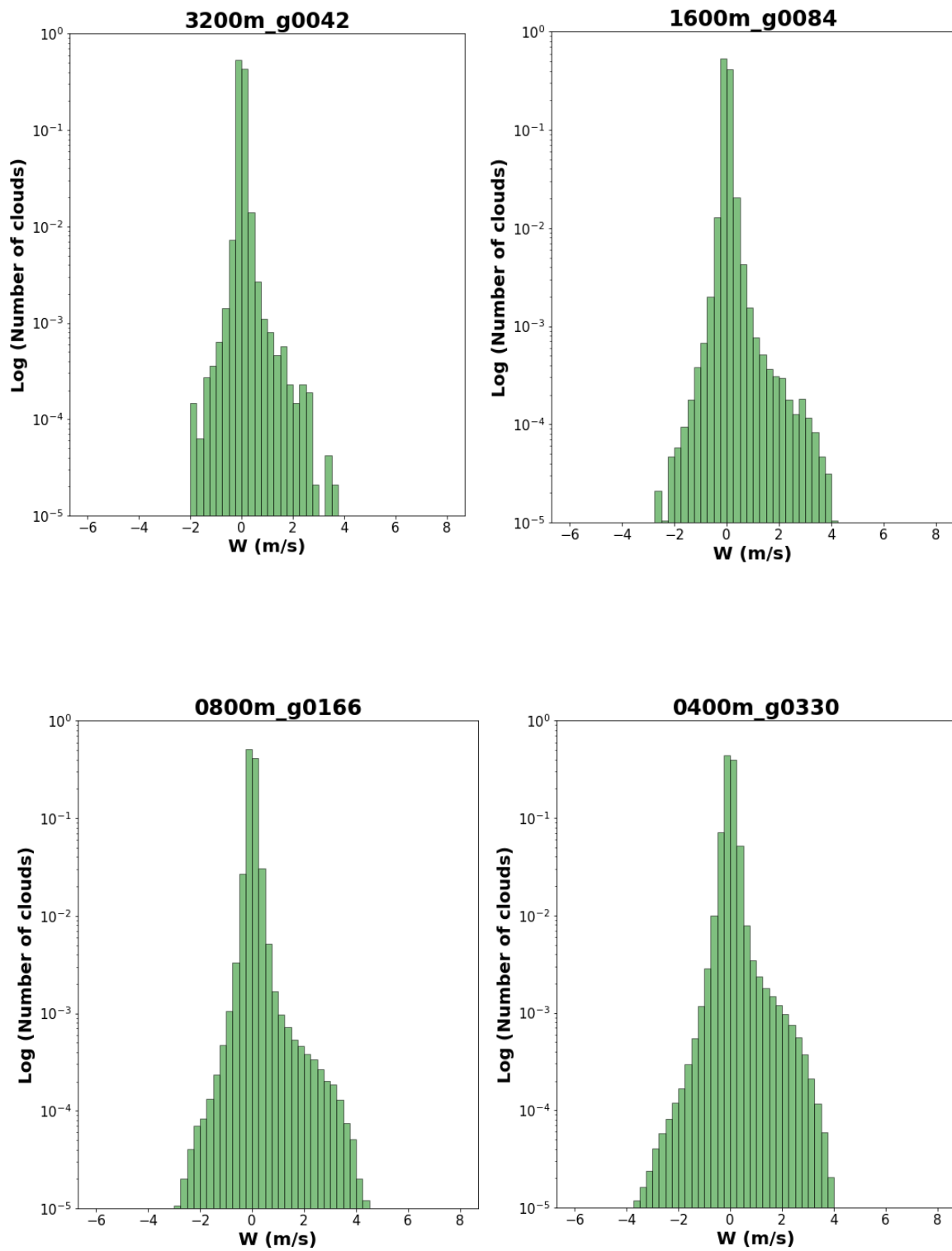


Figure 4.9: Distribution of vertical wind velocity data for 3200, 1600, 800 and 4000 m resolutions in normalized log – space.

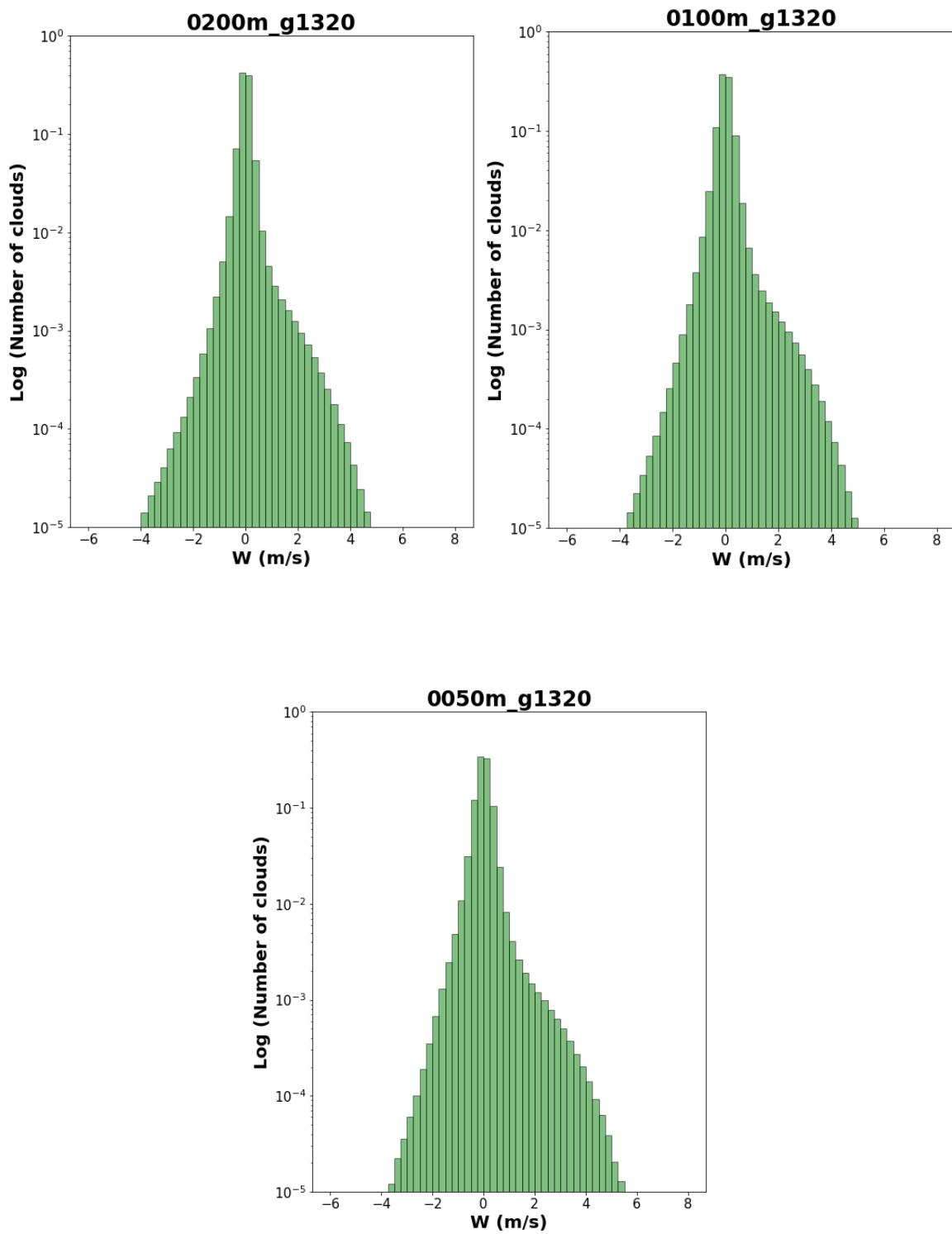


Figure 4.10: Distribution of vertical wind velocity data for 200, 100 and 50 m resolutions in normalized log – space.

4.3 Cloud fraction variation with outputs

Figure 4.11 shows the cloud fraction variation with each timestep. Here, x axis indicates the number of timesteps not the actual time at which the data was taken. Data spans for 2 to 3 days for each resolution (Table 3.1). This give an idea on the variability of data in each time step. Lowest three resolutions showed cloud fraction around 1% and higher variability compared to highest four resolutions with cloud fraction around 4 %. But over all data in balance for all resolutions.

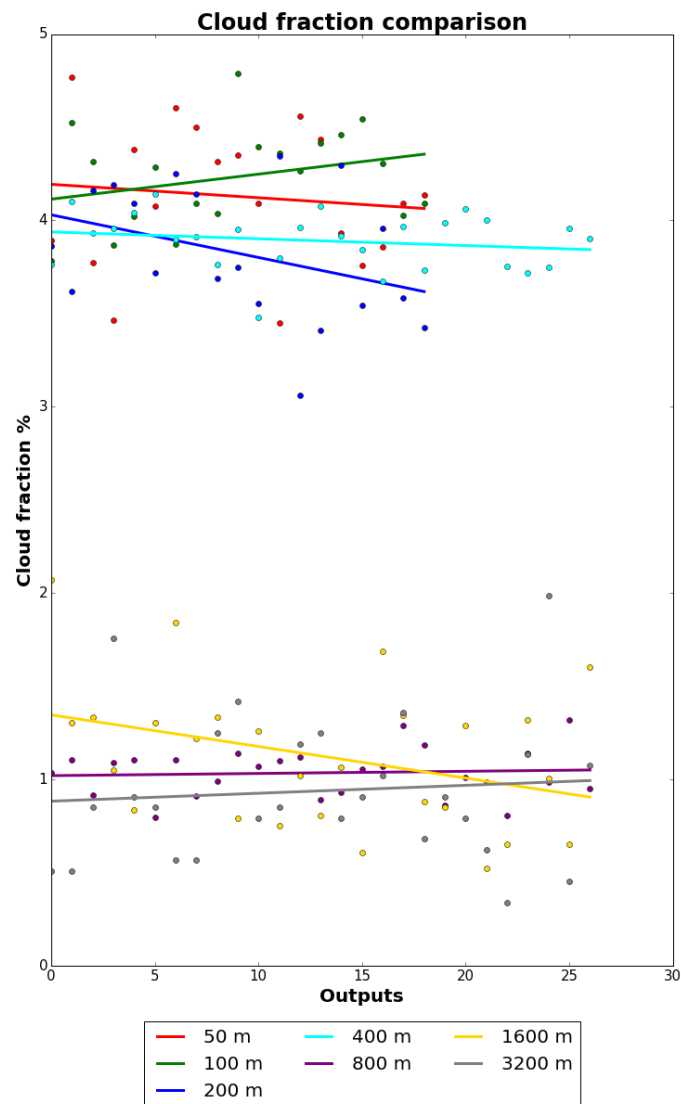


Figure 4.11: Cloud fraction variation for 27 each time steps in 3200 (grey dots), 1600 (yellow dots), 800 (purple dots), 400 (light blue dots) m resolutions and 19 each time steps in 200 (blue dots), 100 (green dots), 50 (red dots) m resolutions. Straight lines show curve fits for each resolution (same colours as dots).

4.4 Cloud identification algorithm

One of the main objectives of this project is to develop a cloud identification algorithm. The programmed procedure is discussed in section 3.3. As mentioned there, main problem with data were raised in the clouds located at the domain edges since the edge properties are connected. Therefore, if there are connecting clouds in the edges, it was important to consider them as a single object.

This algorithm enables us to identify cloud objects, label them accordingly and obtain information on number of objects, number of grid points each object contains, average q_{cl} within each object and the indexes of object positions. Area of the clouds were determined by multiplying number of grid points each object contains by area of one grid point ($dx \times dy$). Object position indexes were used to obtain vertical wind velocity data at same indexes from w NetCDF files. Due to model configurations, q_{cl} and w data have different vertical levels. Therefore, to obtain w data at 842 m vertical level, data from 785 m and 902 m were extracted and averaged since w vertical levels are lying in between q_{cl} vertical levels. Section 4.4 discusses the statistical analysis of these data.

4.5 Sensitivity of equilibrium convective ensemble statistics

In this section cloud properties are evaluated. Cloud number, cloud size, average q_{cl} and w in clouds and $w \times q_{cl}$ were analysed statistically. First, distributions of cloud number and size were investigated because these are important in numerical simulations and parameterizations. Then, the changes in cloud properties were analysed.

4.5.1 Distribution of cloud size

Cumulus cloud size and distribution are very important parameters when studying cloud properties. Arakawa and Schubert (1974) first introduced cumulus cloud size into a parameterization scheme.

Figure 4.12 shows number of clouds obtained for different resolutions. Since the number of outputs are different for each resolution, cloud number percentages for four area thresholds (1, 5, 10 and 20 km²) were considered. According to the figures, the higher the resolution the smaller the number of large clouds. For the highest resolution (50 m), there is very small percentage ($\approx 1\%$) of clouds exceeding area 1km² while 100 % of the clouds observed in 3200 m and 1600 m are larger than 1km². Note that minimum area of the cloud is one grid box size (dx^2) for each resolution. But as discussed in section 4.1.2, average maximum cloud fraction increases from 1.25 % to 4.5 % when resolution increases from 3200 m to 50 m. This implies that even though average size of single cloud decreases with resolutions (Figure 4.12), number of clouds increases strongly with resolution. Since the grid spacing is smaller at higher resolutions, one cloud seen in low resolution can be identified as two different clouds at higher resolution. However as seen in Figure 4.11 which shows best fit curves of cloud fraction variation for each resolution, highest two resolutions have nearly same cloud fraction values. This is clearly seen in Figures 4.13 to 4.19 which shows snapshots of 842 m vertical level cloud distribution for the first output of each resolution. Cloud fraction of three outputs for highest three resolutions shown in figures 4.17, 4.18 and 4.19 are not increasing with resolution even though their values are nearly same. These figures are shown only to give a visual impression on the cloud distribution.

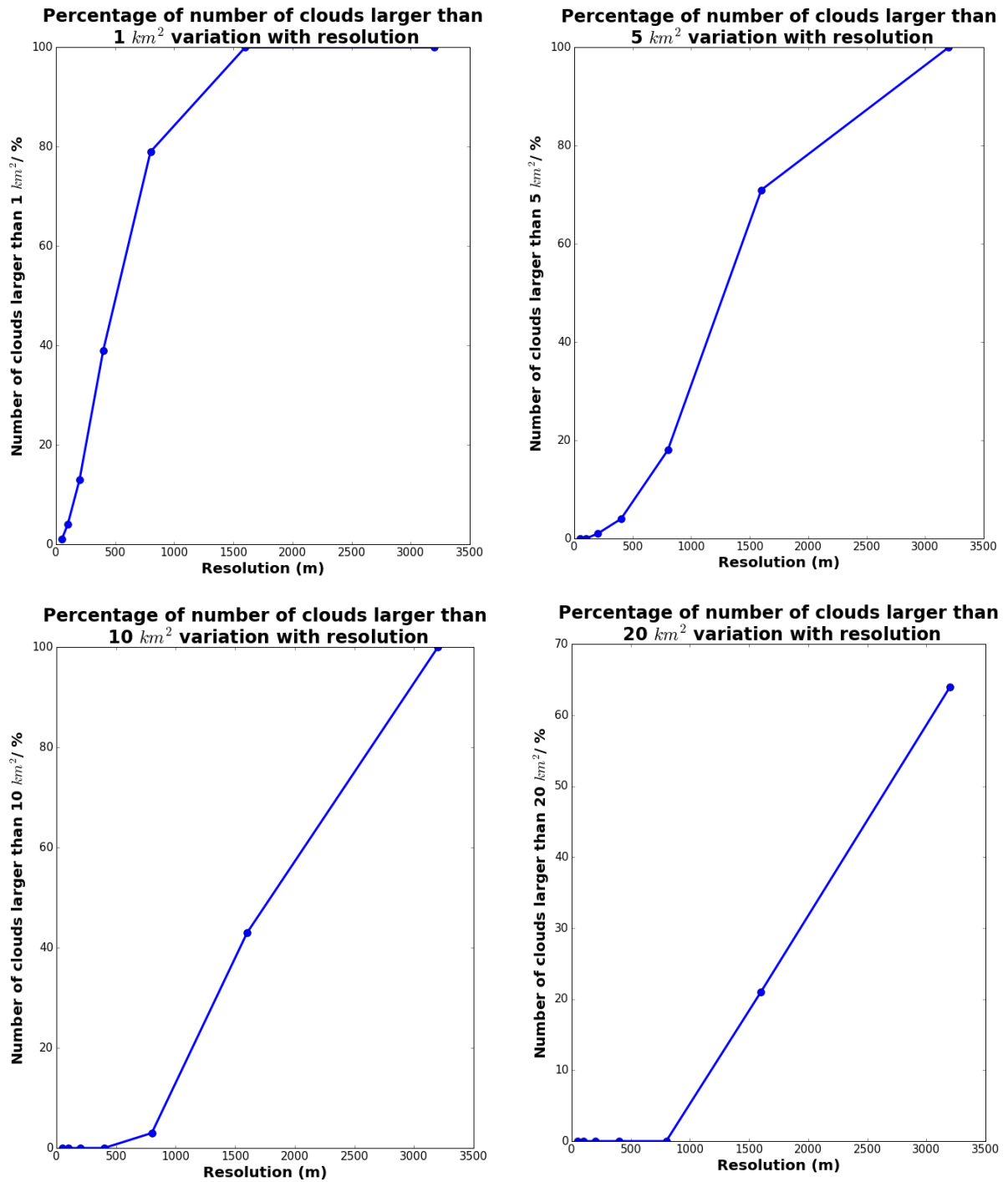


Figure 4.12: Percentage of number of clouds variation with resolution for 1, 5, 10 and 20 km² thresholds.

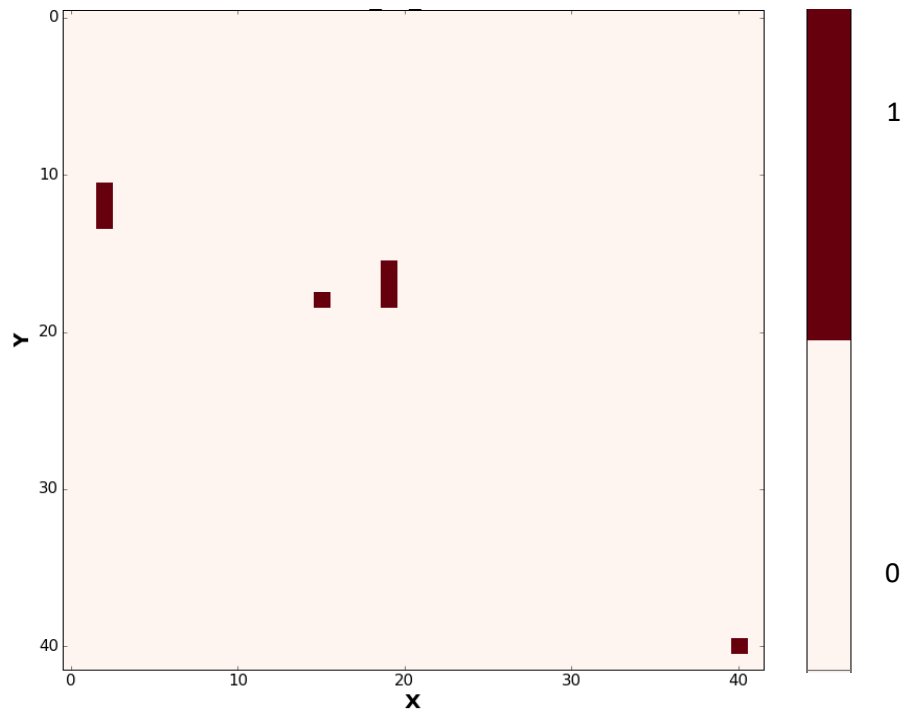


Figure 4.13: Snapshot of 3200m resolution 842 m vertical level first output (cloud fraction = 0.0045)

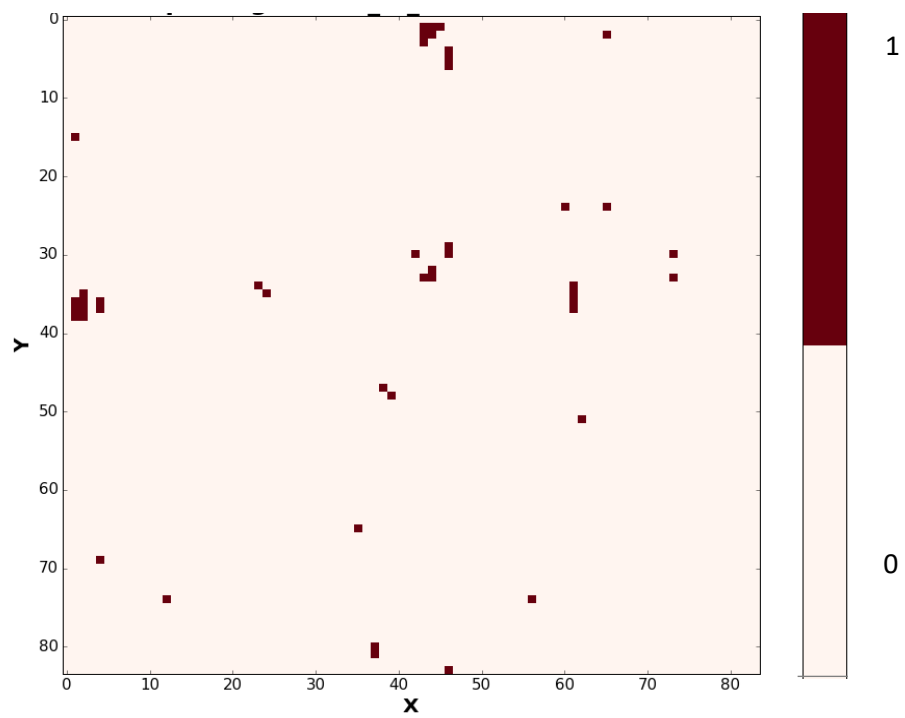


Figure 4.14: Snapshot of 1600m resolution 842 m vertical level first output (cloud fraction = 0.0065)

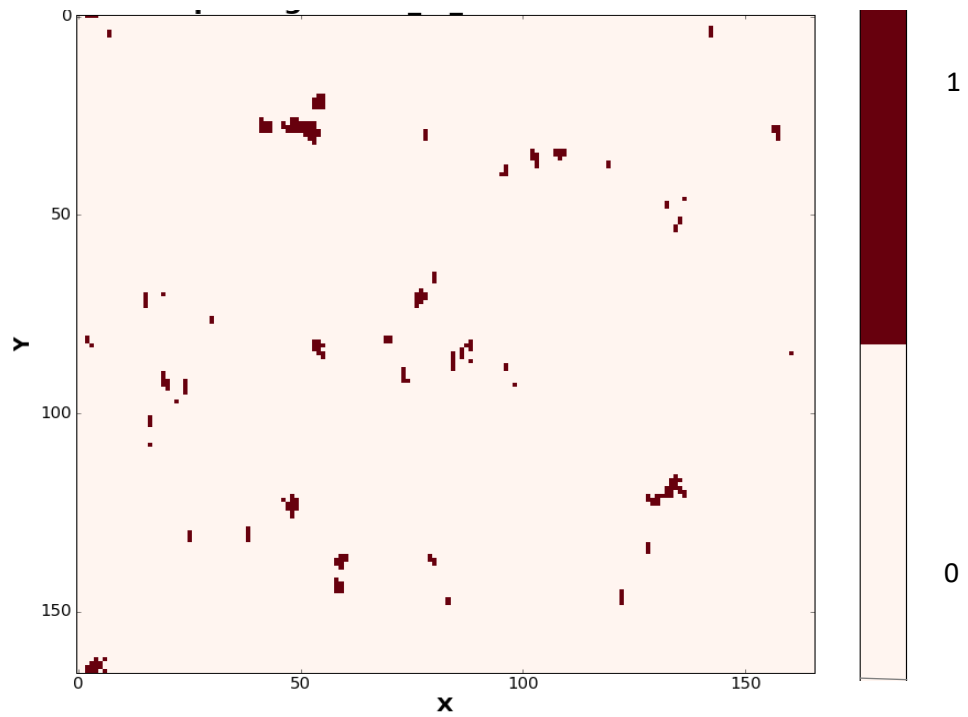


Figure 4.15: Snapshot of 800m resolution 842 m vertical level first output (cloud fraction = 0.0093)

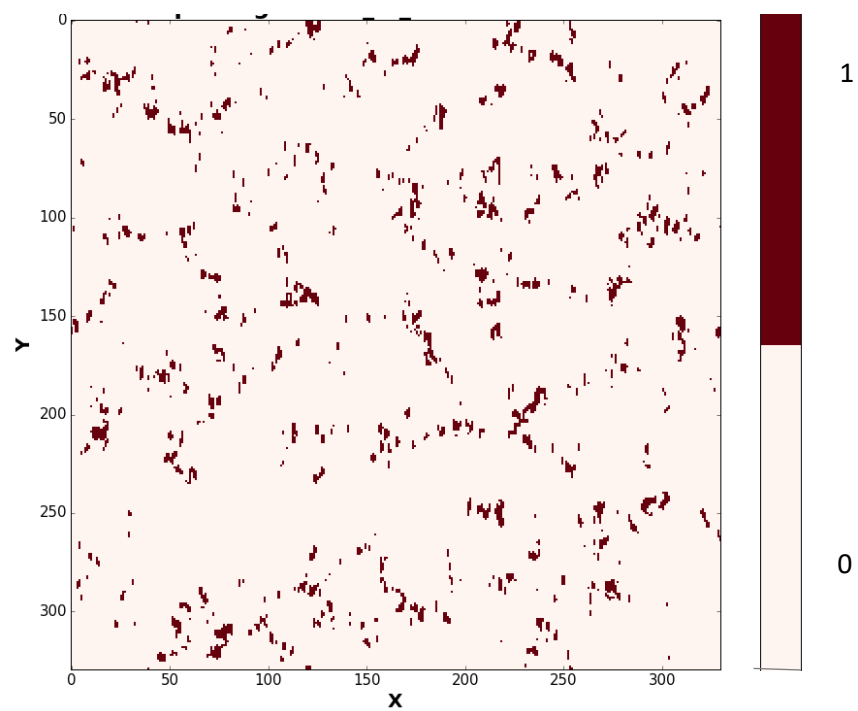


Figure 4.16: Snapshot of 400m resolution 842 m vertical level first output (cloud fraction = 0.0399)

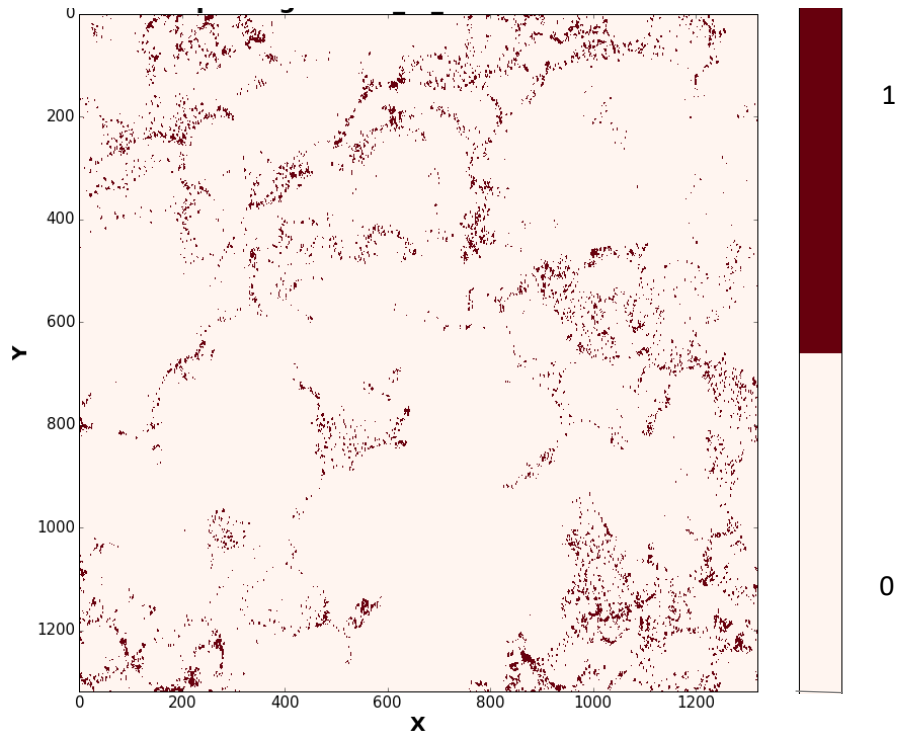


Figure 4.17: Snapshot of 200m resolution 842 m vertical level first output (cloud fraction = 0.0357)

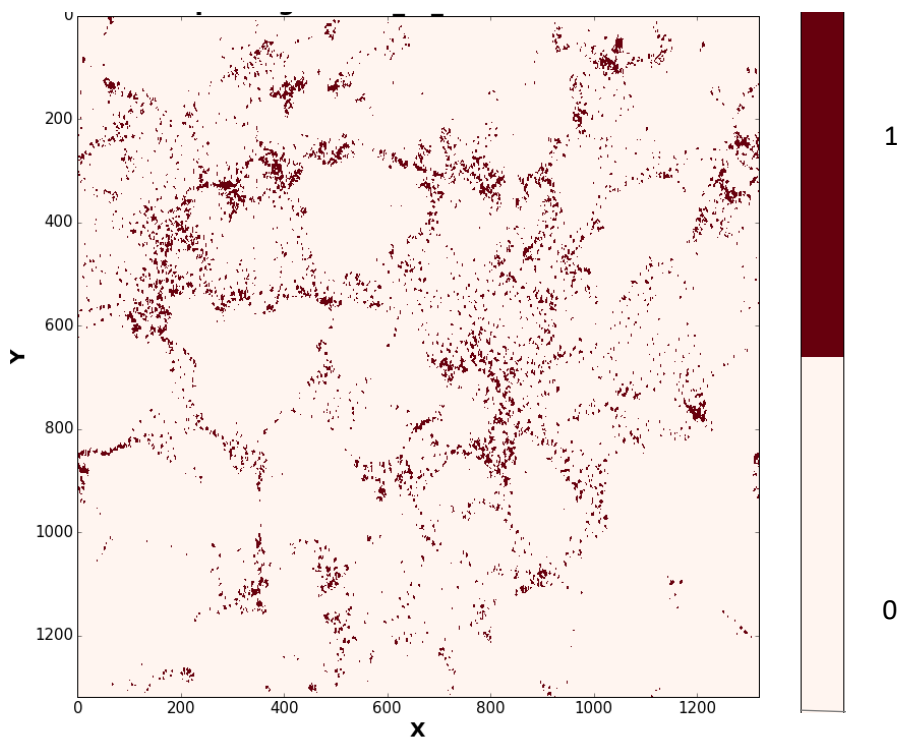


Figure 4.18: Snapshot of 100m resolution 842 m vertical level first output (cloud fraction = 0.0439)

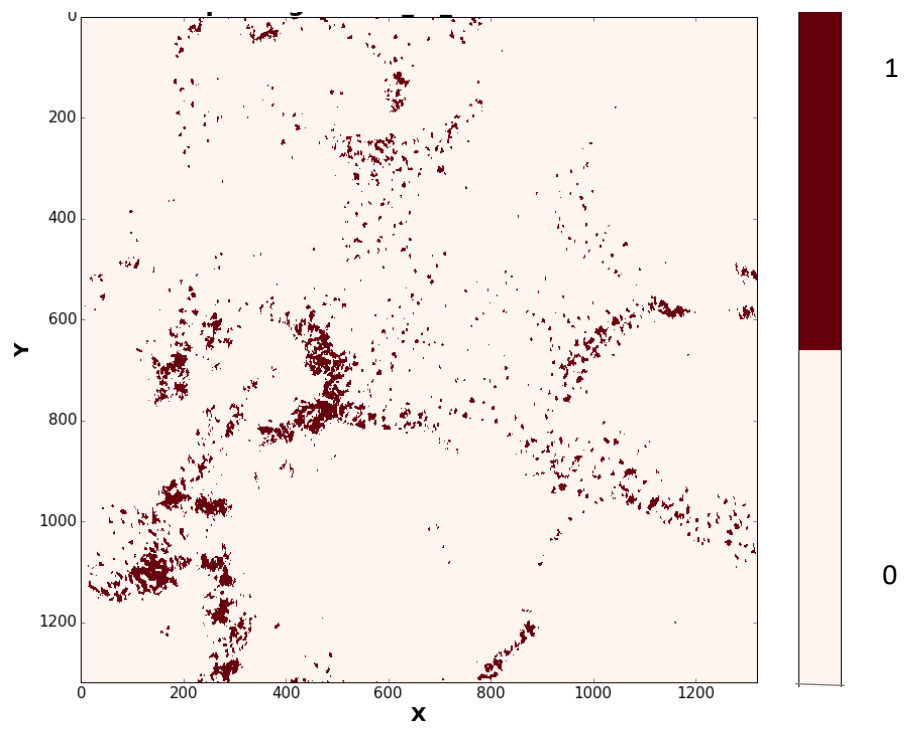


Figure 4.19: Snapshot of 50m resolution 842 m vertical level first output (cloud fraction = 0.0386)

According to early studies, cloud area distributions can be either exponential, log-normal or power law (Scheufele, 2014, Lennard, 2004). Figure 4.20 and 4.21 shows distribution of convective cloud area produced for the seven resolutions in radiative – convective equilibrium. As seen in figures and according to early explanations 3200 m resolution have larger cloud though the cloud fraction is low. Largest clouds are about $1.6 \times 10^2 \text{ km}^2$. Cloud area decreases as resolution increases up to 400 m. But, the trend breaks at this point and 200 m resolution shows some larger clouds. When 3200 m and 50 m resolutions are compared, there is a factor of ten decrease in maximum cloud size which agrees with the results obtained by Scheufele, 2014.

Figure 4.22 shows results obtained by Scheufele, 2014 for radiative cooling -4 K day^{-1} and -12 K day^{-1} used for simulations at resolution 2 km and 125 m. Cloudy grid points were defined where vertical velocity exceeds a threshold of 1 ms^{-1} . These results also show reduction of cloud area for higher resolutions. Even though the radiative cooling used is much higher than the value used in this study (1.5 K day^{-1}), they agree with the results. Specially in -4 K day^{-1} simulations, cloud areas are in the same order of 1600 m and 100 m resolutions.

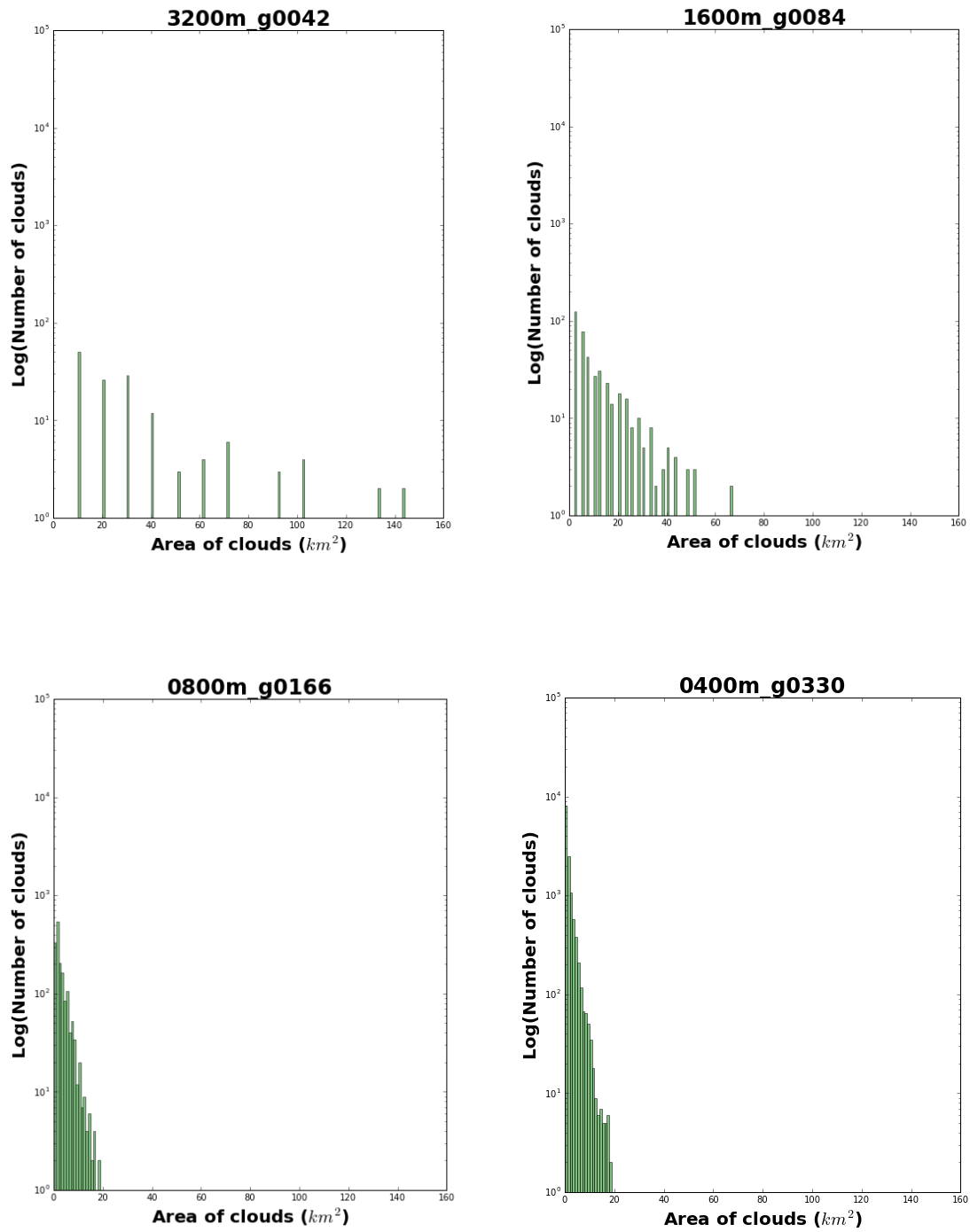


Figure 4.20: Distribution of cloud area for 3200, 1600, 800 and 400 m resolutions in log – linear space.

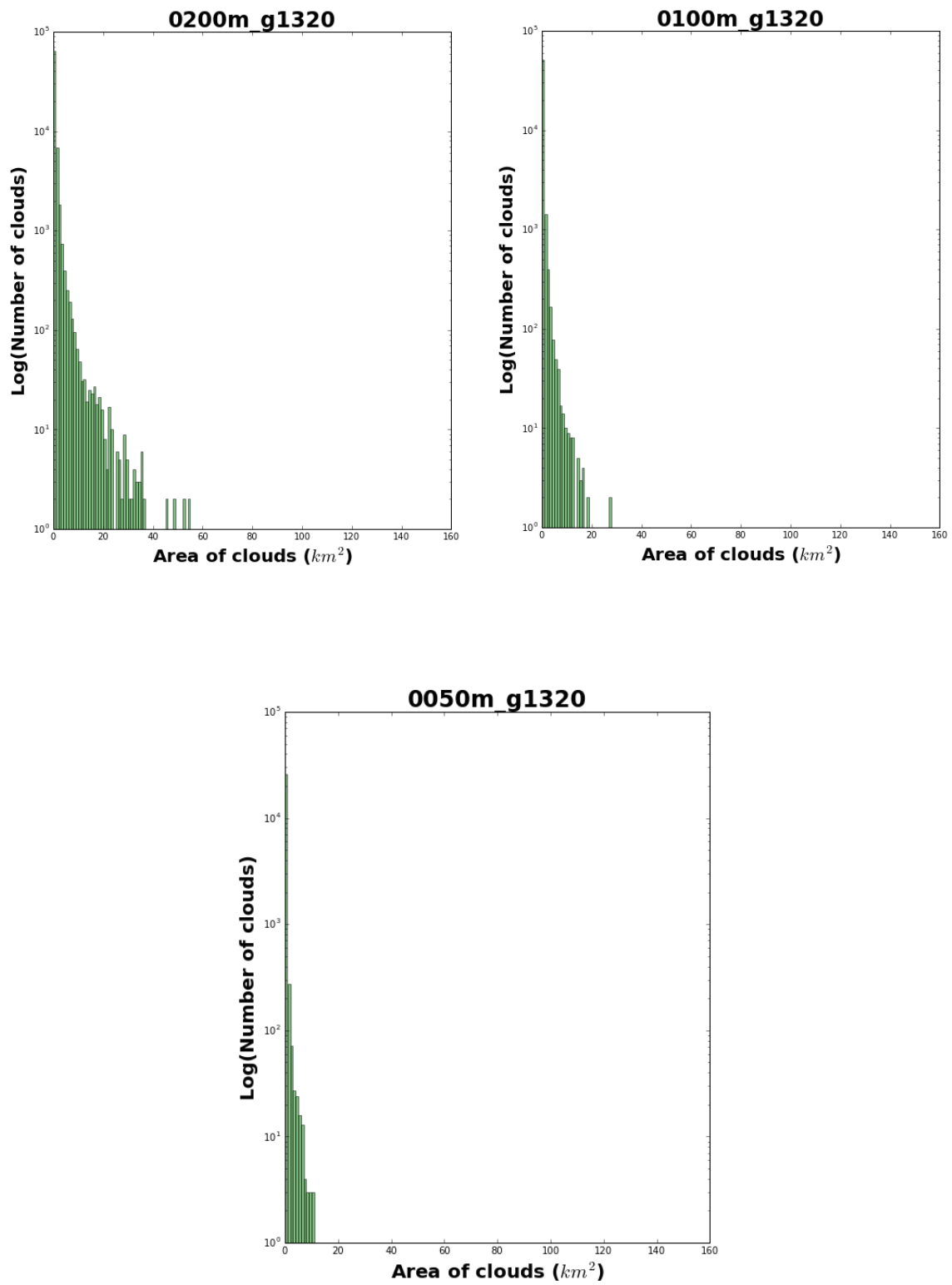


Figure 4.21: Distribution of cloud area for 200, 100 and 50 m resolutions in log – linear space.

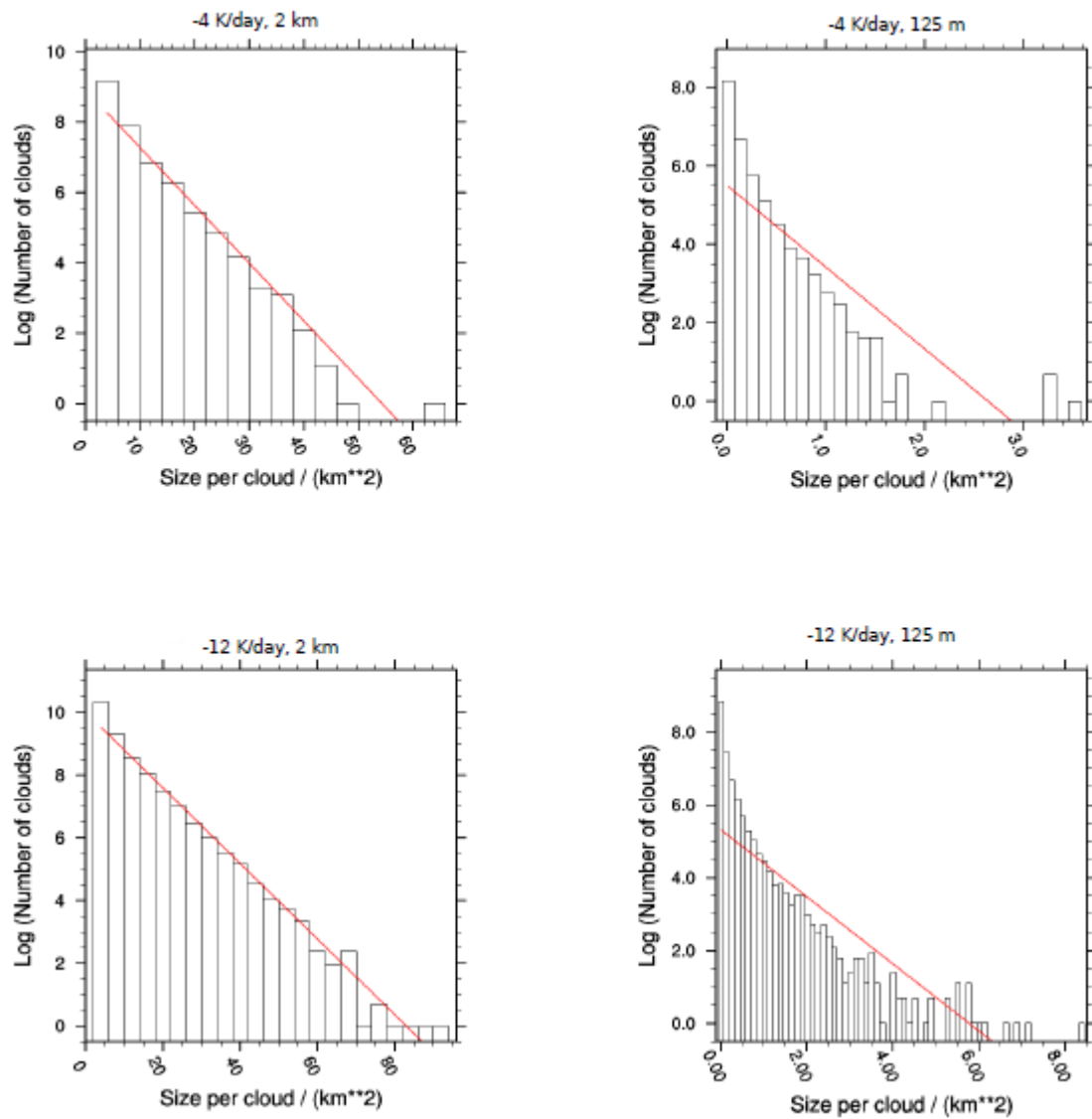


Figure 4.22: Cloud area distribution in log – linear space for -4 K day^{-1} and -12 K day^{-1} simulations at 2 km and 125 m resolutions (red lines shows the least square best fit) (Scheufele, 2014).

4.5.2 Average cloud liquid water content

Average liquid water content per cloud was extracted using object identification algorithm. The distribution is shown in Figure 4.23 and 4.24. The highest average LWC of clouds varies between $5 - 7 \times 10^{-4}$ kg/kg for all resolution except for 800 m resolution where highest values are in the range of 4×10^{-4} kg/kg. There is no significant variation of average cloud LWC in any resolution. However, distributions for lower four resolutions (Figure 4.23) are more 'flatter' compared to higher three resolutions (Figure 4.24) i.e., q_{cl} variation is more even at low resolution compared to higher resolutions where low q_{cl} is quite common and the high q_{cl} is relatively rare. This may be due to larger clouds observed in the lowest two resolutions. When the highest values of LWC is compared with the values shown in section 4.2.1 (Figures 4.6 and 4.7), 3200 m and 1600 m resolutions show same values but for 100 m and 50 m, cloud average LWC do not reach the highest values of LWC in the total dataset. This may have a connection with the cloud area as it decreases significantly with resolution.

In this study, cloud positions identified where q_{cl} is larger than 1×10^{-6} kg/kg. This threshold can was selected by comparing the snapshots at 842 m vertical level since the cloud identification algorithm was not developed at the time. Further, the vertical level selected for the study is agreeing more for higher resolutions. Therefore, it would be useful to study further the average LWC variation of clouds for different thresholds and for different vertical levels to have better idea of cloud LWC.

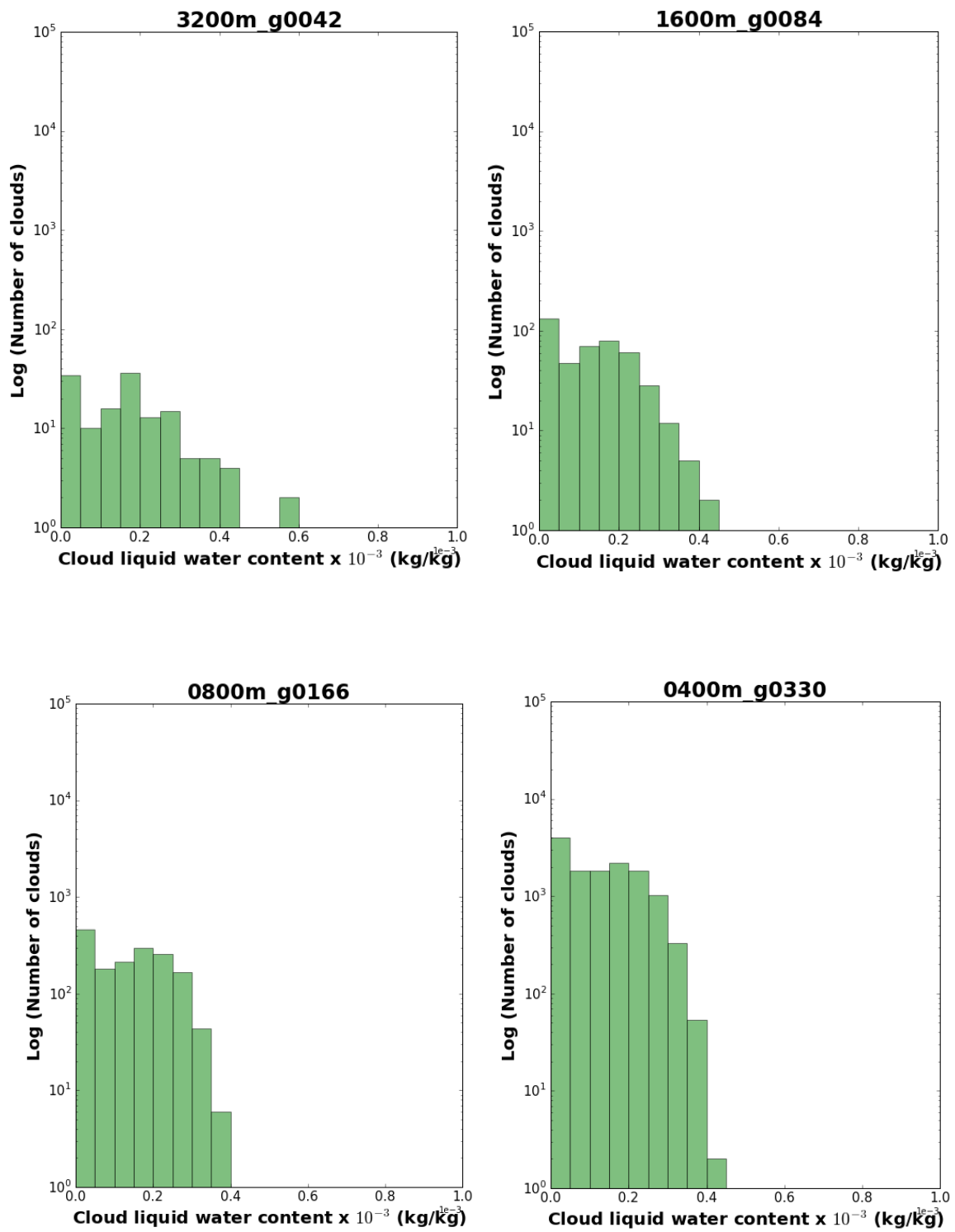


Figure 4.23: Average cloud liquid water content distribution for 3200, 1600, 800, 400 m resolutions in log- linear space.

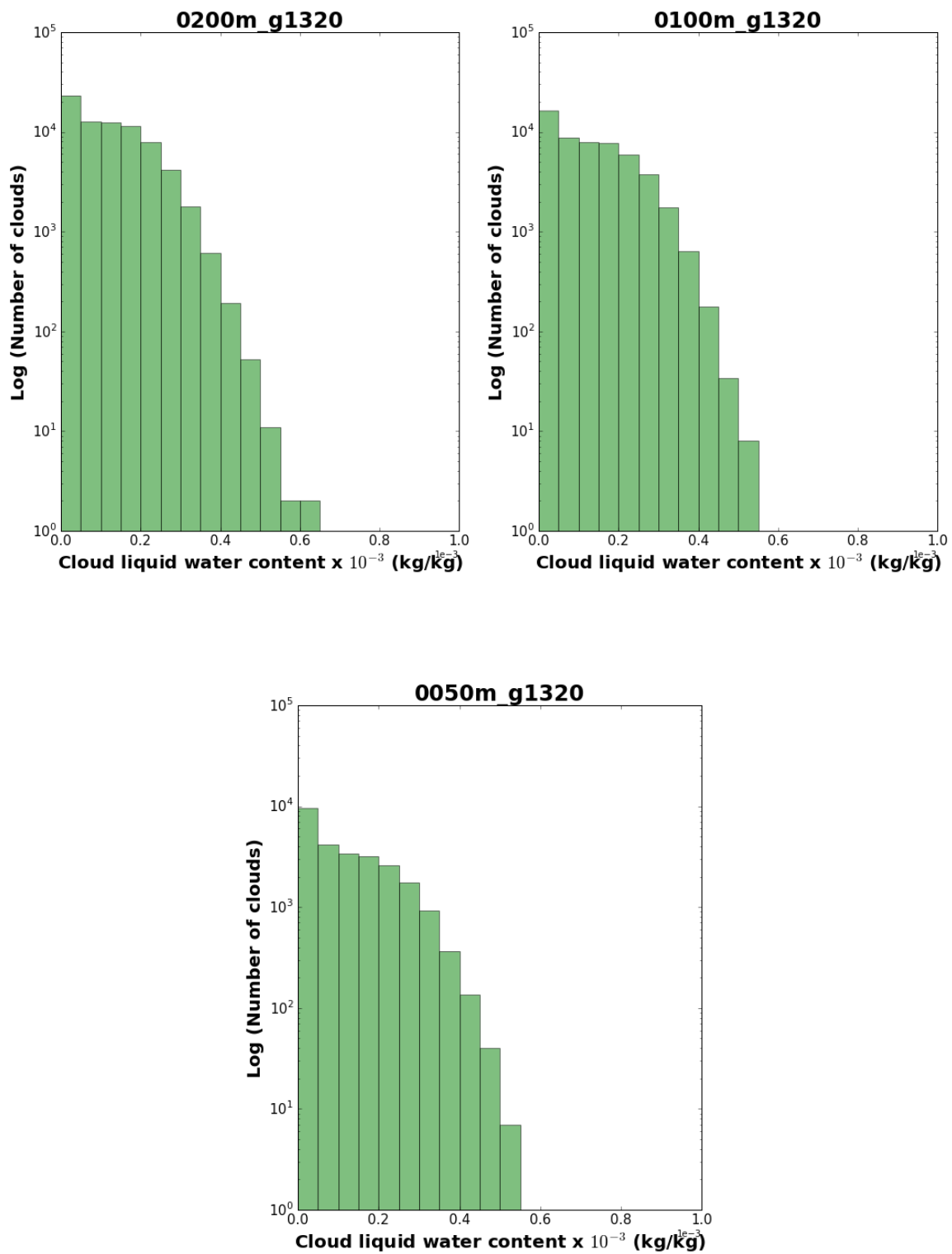


Figure 4.24: Average cloud liquid water content distribution for 200, 100, 50 m resolutions in log- linear space.

4.5.3 Average vertical wind velocity

Average vertical wind velocities were obtained for the same locations of clouds identified using cloud LWC data. Since LWC and vertical wind velocity data have different vertical levels, to obtain data at 842 m level, 921 m and 785 m values were averaged. As seen in Figures 4.25 and 4.26, none of the resolutions have values more than 2 ms^{-1} . When comparing vertical wind velocities, analysis height is important as for deep and very active clouds, w increases with height from cloud base and reduces again only towards the top of the cloud. In this study, 842 m vertical level was considered. Since it is not far away from cloud base very high vertical wind velocities cannot be expected. Scheufele, 2014 used 1 ms^{-1} as the threshold to identify simulated clouds while Yang et al. 2016 used 0.2 ms^{-1} for in-situ data observed from an aircraft at three field campaigns: High-Plains Cumulus (HiCu) conducted over the mid-latitude High Plains, Convective Precipitation Experiment (COPE) conducted in a mid-latitude coastal area, and Ice in Clouds Experiment-Tropical (ICE-T), conducted over a tropical ocean. Figure 4.24 shows the data observed by Yang et al. 2016 which indicates that study also observed more vertical wind velocity in the range of -2 to 2 ms^{-1} . Even though 3200, 1600, 800 and 400 m resolutions, most of the clouds shows updrafts, 200 m, 100 m and 50 m resolutions show more symmetric distributions of updrafts and downdrafts.

It will be better to use vertical wind velocity threshold to identify clouds and compare the locations with the data obtained from this study. It will give a better understanding on whether both results show same locations for cloudy points.

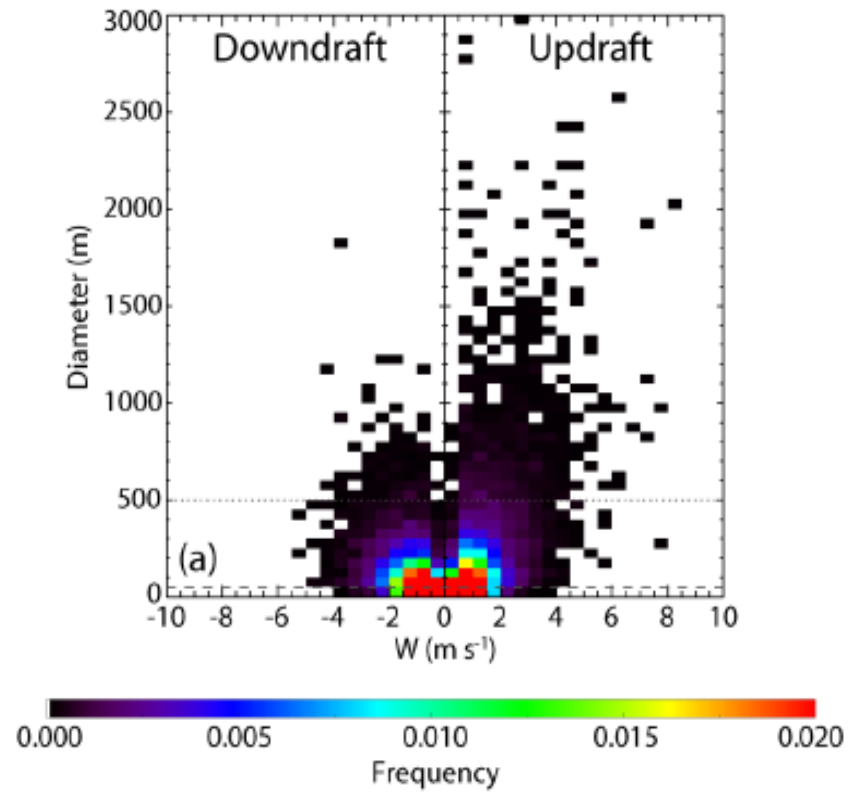


Figure 4.24: Occurrence distributions as a function of diameter and mean vertical velocity at cloud height between 0 to 8 km (Yang et al. 2016).

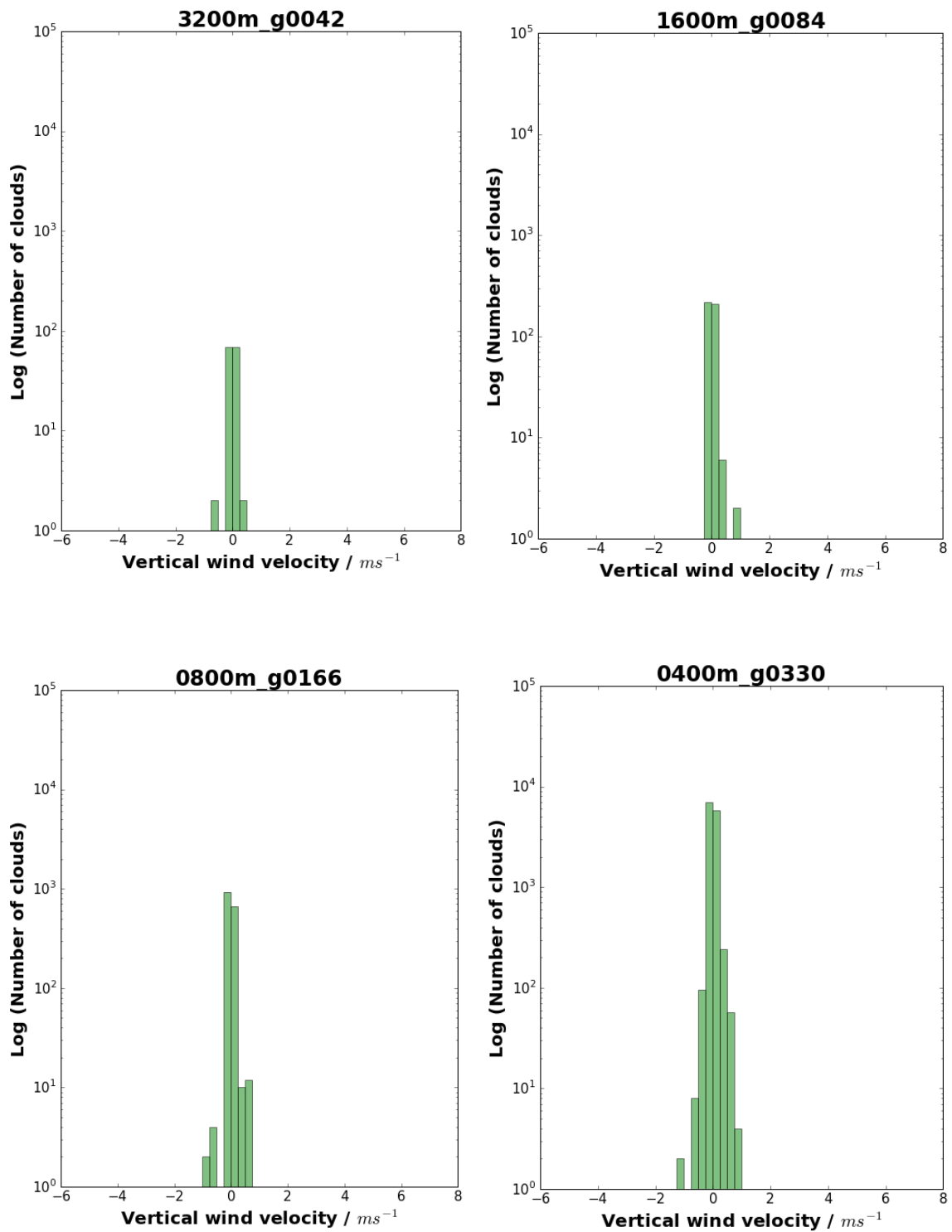


Figure 4.24: Cloud average vertical wind velocity distribution for 3200, 1600, 800, 400 m resolutions in log-linear space.

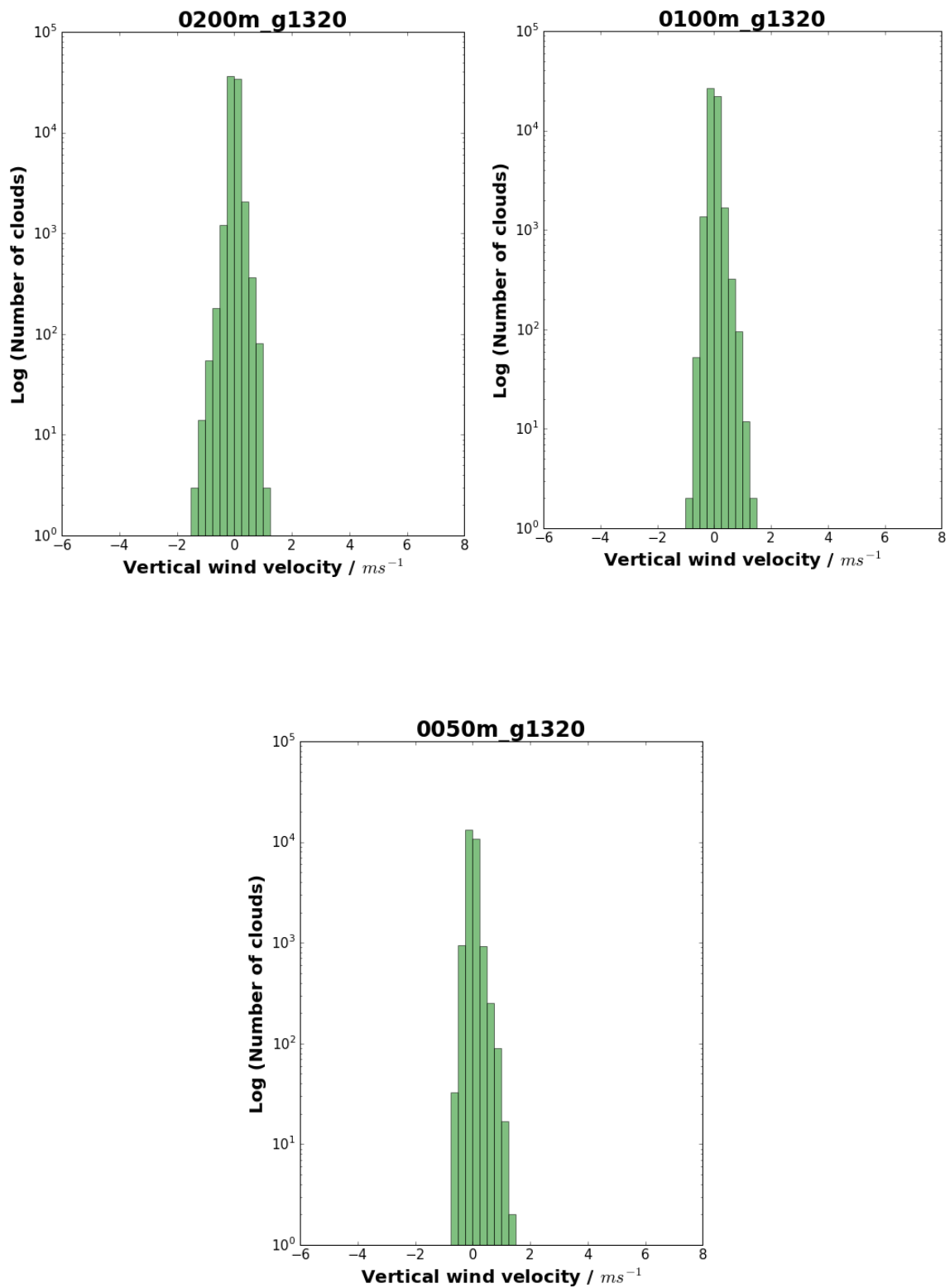


Figure 4.25: Cloud average vertical wind velocity distribution for 200, 100 and 50 m resolutions in log-linear space.

4.5.4 Distribution of cloud liquid water flux

Liquid water flux was calculated by multiplying cloud liquid water content by cloud vertical wind velocity. This explains the liquid water transportation within clouds. Figures 4.26 and 4.27 shows the distribution of liquid water flux for seven resolutions. As discussed in section 4.4.3, higher the resolution, larger the amount of clouds with downdraft. Therefore, more downward motion of liquid water can be seen in higher resolutions. When the figures are compared, 400 m resolution acts more like higher resolutions compared to the lowest three resolutions.

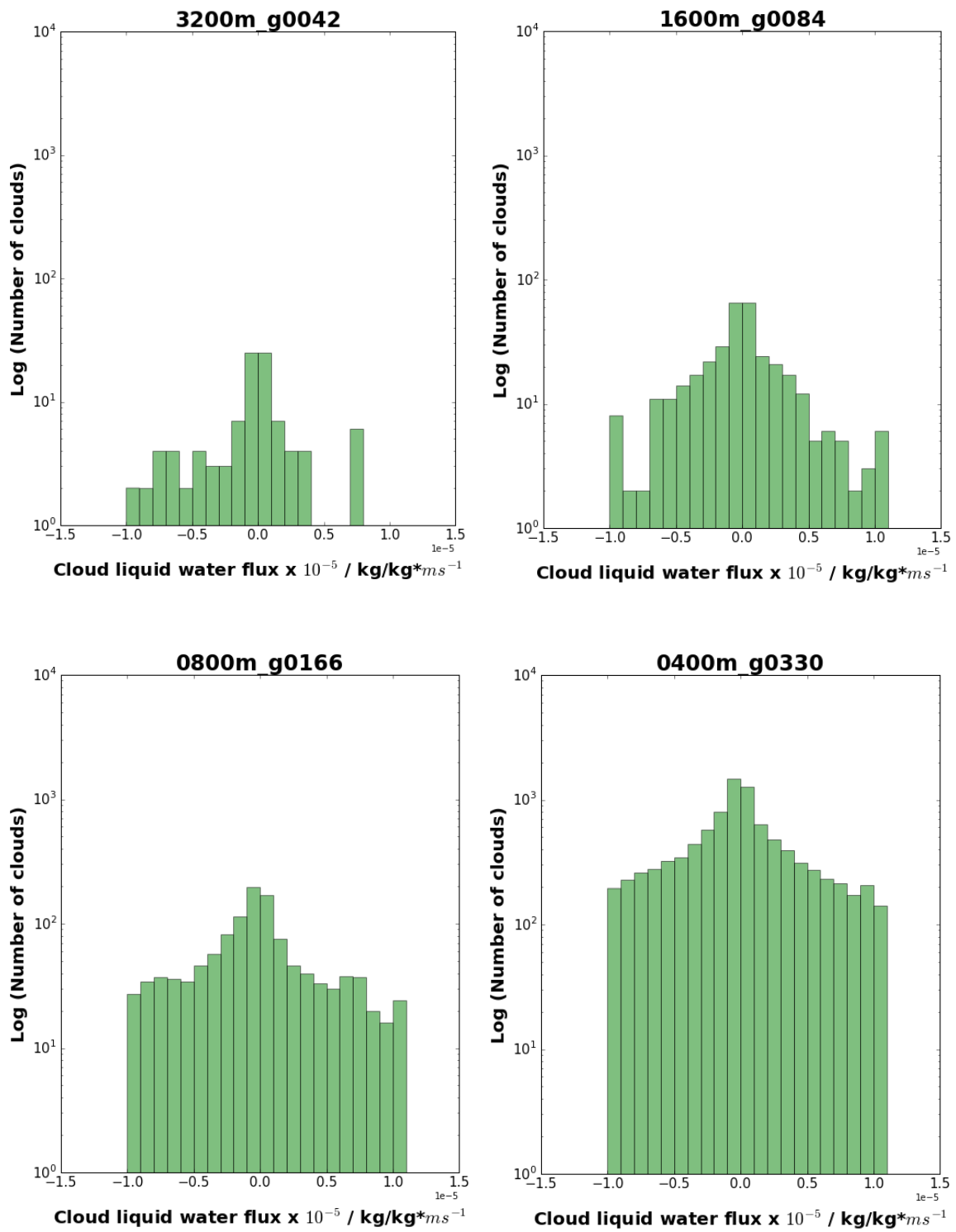


Figure 4.26: Cloud average mass flux distribution for 3200, 1600, 800 and 400 m resolutions in log- linear space.

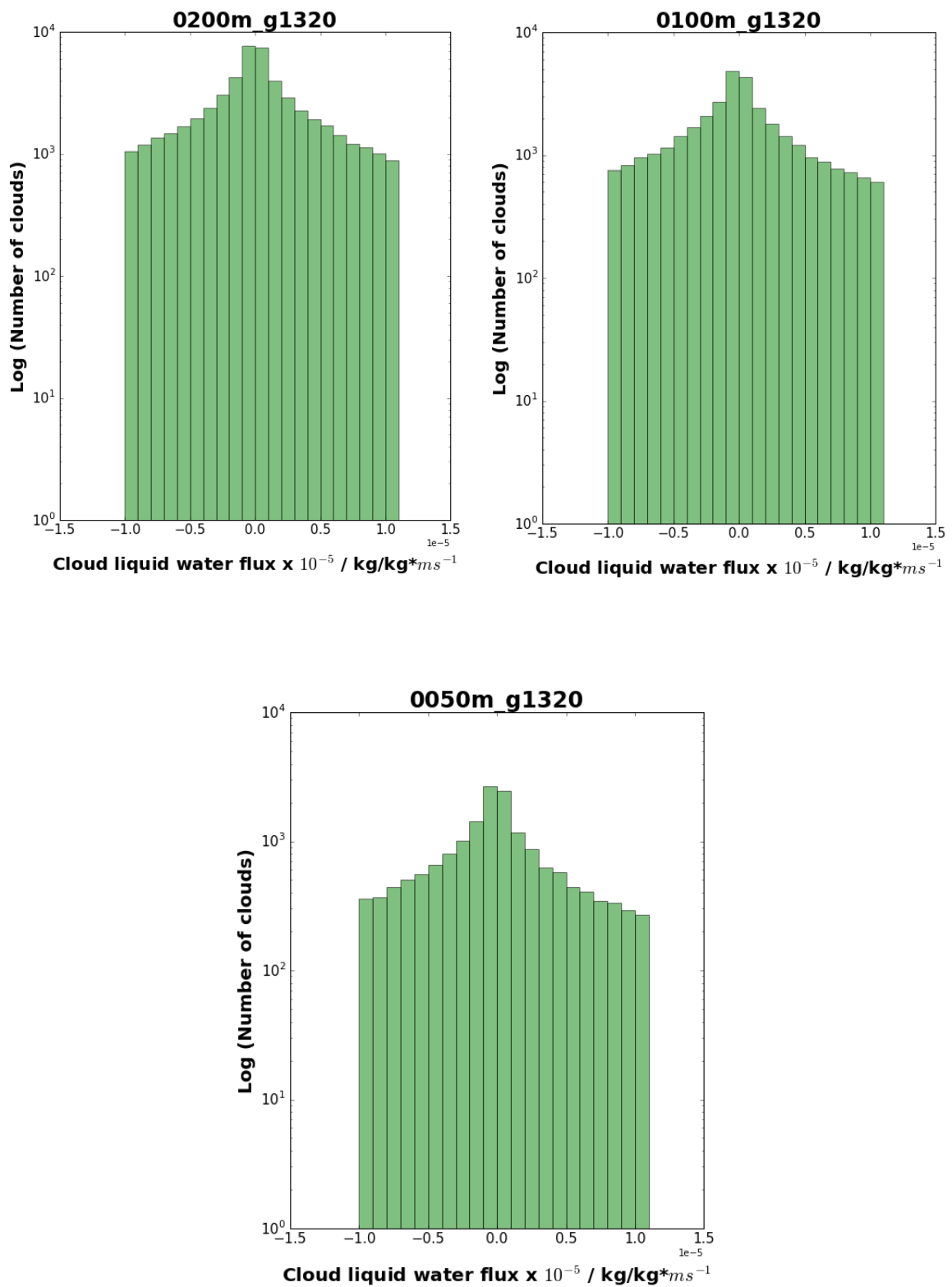


Figure 4.26: Cloud average liquid water flux distribution for 200, 100 and 50 m resolutions in log- linear space.

5. Summary, Conclusion and Future work

5.1 Summary

The main object of this dissertation is to identify the best resolution which can be used with confidence to study convergence properties of convective clouds simulated using Met Office – NERC high resolution large eddy model, MONC. Data consist of cloud liquid water content and vertical wind velocity obtained for seven different resolutions 3200, 1600, 800, 400, 200, 100 and 50 m.

First, it was important to determine a height level for further analysis. Therefore, average LWC and cloud fraction variation with height were plotted for all resolutions. Both graphs disclosed significant increase of LWC and cloud fraction with increasing resolution. 3200 and 1600 m resolutions exhibited similar values. Subsection 4.3.1 discussed the variation of LWC. Two different vertical levels were identified for maximum LWC where for lowest three resolutions 1752 m and for highest four resolutions at 1095m.

To conclude a suitable height level, cloud fraction variation was plotted which indicated highest cloud fraction at 842 m for highest four resolutions and nearly same vertical level for other three resolutions. These results agreed with the published data.

Then, probability distribution was plotted for LWC and vertical wind velocity (subsections 4.2.1 and 4.2.2). For both quantities, 3200, 1600 and 800 m resolutions exhibited similar behaviours while 200, 100 and 50 m resolutions behaved similar. 400 m showed a mixed behaviour of lowest three resolutions and highest three resolutions. Distribution was more symmetric for vertical wind velocity 3200 m resolution and it becomes more asymmetric for increasing resolutions. It shows more points with higher updrafts in higher the resolution.

Second main objective of this study is to develop and cloud identification algorithm. Main problem was with the clouds at the edges since wrap – around boundary conditions are been used in the simulations. On the data set, first row was connected to last row and first column with the last column. Therefore, measures should be taken to algorithm to identify connecting clouds on the edges as one object. This was performed by developing a program in python, which compare the grid point coordinates on edges and corners of the domain for connected clouds. If there are neighbouring clouds it will identify it as a one object. For an identified cloudy grid point, if the algorithm identifies another cloudy grid point at one of the eight surrounding grid points, both will identify as same object.

Number of clouds, area of clouds, average LWC and average vertical wind velocities were extracted using the algorithm and average mass flux of clouds were determined using LWC and vertical wind velocity data extracted. Distribution of cloud sizes were discussed in subsection 4.4.1. 3200 m resolution have the largest clouds where all of them have sizes more than 10 km^2 while number of large clouds per resolution decreases with increasing resolution. Snapshots of 842 m vertical level shows better visual indication. There is a tenfold reduction of cloud area in 50 m resolution compared to 3200 m which agrees with previous studies.

Average LWC within the clouds did not show a significant change over resolution. 100 m and 50 m resolutions had more clouds with smaller average LWC. Vertical wind velocity and LWC data were simulated at different vertical levels in the model run. Therefore, to obtain data for 842 m level, 902 m and 785 m levels of vertical wind velocities were averaged. Histograms showed all average vertical wind velocities of clouds are lying within the range of -2 to 2 m s^{-1} which is smaller than the values recorded in previous studies. 3200, 1600, 800 and 400 m resolutions show more updrafts while 200, 100 and 50 m exhibits more symmetric histograms with both updrafts and downdrafts.

5.2 Conclusions and limitations

First objective of this dissertation is to determine a suitable vertical level investigate cloud properties. This was achieved by analysing cloud LWC and cloud fraction variations with height. 842 m vertical level was chosen as the vertical level for the analysis. Since vertical wind velocity data were obtained for different vertical levels, data in 902 m and 785 m levels were averaged.

PDFs were plotted to investigate the reproducibility of data in coarse resolutions. According to the results, model is capable of reproducing LWC and vertical wind velocity data at high resolutions. Higher the resolution more data can be extracted. 200, 100 and 50 m behave in same manner while 3200, 1600 and 800 m resolution data behave the same. 400 m resolution behave in mixed manner of lower and higher resolutions.

Cloud identification algorithm can successfully identify clouds where LWC is larger than 1×10^{-6} kg/kg and extract number of clouds, area, average LWC and vertical wind velocity of each cloud. Cloud area decreases significantly while the number of large clouds decreases with resolution. Only 3200 m resolution contain clouds larger than 10 km^2 . There is no significant variation of average cloud LWC with resolution. But for highest three resolutions, there are more clouds with smaller average LWC values.

Average wind velocities were smaller than expected. They were within the range of -2 to 2 ms^{-1} . 3200, 1600, 800 and 400 m distributions are asymmetric with more updraft winds while distributions are more symmetric for other resolutions with both updrafts and down drafts.

According to the analysis, 200, 100 and 50 m resolutions exhibits similar variations. Therefore, 200 m is a better resolution to use for further analysis with confidence as most of the properties converge at this resolution. However, this selection can vary with the physical property been investigated. For example, 400 m resolution can be used to investigate downdraft properties of clouds.

Main limitation of this study is that these data are only valid for RCE runs. Therefore, it is better to analyse these properties in more diagnostics of coarse.

5.3 Future work

Since clouds are very small due to the discontinuity in three highest resolutions 200, 100 and 50 m, it is better to increase the neighbourhood structure to 5×5 matrix or higher so that high – resolution data can be averaged onto a low -resolution grids before comparing. This method is known as coarse – graining technique (ECMWF, 2011 and Frenkel et al. 2012) Then the number of clouds per unit area can be compared as the domain sizes are not the same. It will be a better indication to determine whether cloud area distribution follows log-normal, exponential, single power law or double power law.

It will be interesting to identify clouds using vertical wind velocity data with a suitable threshold and check average LWC values, area of clouds and locations of clouds so that they can be compared with the results obtained so far. It is also possible to identify clouds using different definitions such as rising, buoyant or integrated LWC.

Standard deviations of data in each timestep can be investigated to have a better idea of the simulation outputs. It will be also interesting to investigate cloud distance and perimeters distribution too. All these analyses can be performed for different heights as different resolutions showed different height levels for maximum average LWC and cloud fractions. Also, different forcing such as stronger forcing with vertical wind shear can be applied to investigate variations of outputs. Statistical quantities in domains such as thermodynamic quantities or measures of turbulence, that could be resolved on the scale of a GCM grid box can also be related.

6. References

- Arakawa, A., and W. Schubert, 1974: Interaction of a Cumulus Cloud Ensemble with the Large-Scale Environment, Part I. *Journal of the Atmospheric Sciences*, 31, 674-701, doi:10.1175/1520-0469(1974)031<0674:ioacce>2.0.co;2.
- Arakawa, A., 2004: The Cumulus Parameterization Problem: Past, Present, and Future. *Journal of Climate*, 17, 2493-2525, doi:10.1175/1520-0442(2004)017<2493:ratcpp>2.0.co;2.
- Brown, N., M. Weiland, A. Hill, B. Shipway, C. Maynard, T. Allen, and M. Rezný, 2015: A highly scalable Met Office NERC Cloud model. *3rd International Conference on Exascale Applications and Software*, 132-137.
- Cahalan, R., and J. Joseph, 1989: Fractal Statistics of Cloud Fields. *Monthly Weather Review*, 117, 261-272, doi:10.1175/1520-0493(1989)117<0261:fsocf>2.0.co;2.
- Calheiros, A., and L. Machado, 2014: Cloud and rain liquid water statistics in the CHUVA campaign. *Atmospheric Research*, 144, 126-140, doi:10.1016/j.atmosres.2014.03.006.
- Charalambous, G., 2017: Evaluating the organisation of convective clouds. University of Reading, UK.
- Clark, P., N. Roberts, H. Lean, S. Ballard, and C. Charlton-Perez, 2016: Convection-permitting models: a step-change in rainfall forecasting. *Meteorological Applications*, 23, 165-181, doi:10.1002/met.1538.
- Devasthale, A., and M. Thomas, 2012: Sensitivity of Cloud Liquid Water Content Estimates to the Temperature-Dependent Thermodynamic Phase: A Global Study Using CloudSat Data. *Journal of Climate*, 25, 7297-7307, doi:10.1175/jcli-d-11-00521.1.
- ECMWF.int, 2011: Accessed August 7, 2018.
<https://www.ecmwf.int/sites/default/files/elibrary/2011/10938-improving-complex-models-through-stochastic-parameterization-and-information-theory.pdf> .
- Emanuel, K., 1994: *Atmospheric convection*. Oxford University Press, Oxford.
- Fosser, G., L. Kendon, and S. Chan, Advantages and disadvantages of convection permitting scales in the representation of precipitation.

- Frenkel, Y., A. Majda, and B. Khouider, 2012: Using the Stochastic Multicloud Model to Improve Tropical Convective Parameterization: A Paradigm Example. *Journal of the Atmospheric Sciences*, 69, 1080-1105, doi:10.1175/jas-d-11-0148.1.
- Giangrande, S. et al., 2016: Convective cloud vertical velocity and mass-flux characteristics from radar wind profiler observations during GoAmazon2014/5. *Journal of Geophysical Research: Atmospheres*, 121, 12,891-12,913, doi:10.1002/2016jd025303.
- Guichard, F., and F. Couvreux, 2017: A short review of numerical cloud-resolving models. *Tellus A: Dynamic Meteorology and Oceanography*, 69, 1373578, doi:10.1080/16000870.2017.1373578.
- Gray, M., 2003: The use of a cloud resolving model in the development and evaluation of a probabilistic forecasting algorithm for convective gusts. *Meteorological Applications*, 10, 239-252, doi:10.1017/s1350482703003049.
- Ilotoviz, E., and A. Khain, 2016: Application of a new scheme of cloud base droplet nucleation in a spectral (bin) microphysics cloud model: sensitivity to aerosol size distribution. *Atmospheric Chemistry and Physics*, 16, 14317-14329, doi:10.5194/acp-16-14317-2016.
- Inness P., Dorling S., 2013: *Operational Weather Forecasting*, Wiley-Blackwell, 231 pp.
- Liu, C. and Zipser, E. (2005). Global distribution of convection penetrating the tropical tropopause. *Journal of Geophysical Research*, 110(D23).
- Lennard, R., 2004: The distribution of cumulus cloud sizes. University of Reading, UK.
- López, R., 1977: The Lognormal Distribution and Cumulus Cloud Populations. *Monthly Weather Review*, 105, 865-872, doi:10.1175/1520-0493(1977)105<0865:tldacc>2.0.co;2.
- Machado, L., and W. Rossow, 1993: Structural Characteristics and Radiative Properties of Tropical Cloud Clusters. *Monthly Weather Review*, 121, 3234-3260, doi:10.1175/1520-0493(1993)121<3234:scarp>2.0.co;2.
- Manabe, S., 1969: climate and the ocean circulation1. *Monthly Weather Review*, 97, 739-774, doi:10.1175/1520-0493(1969)097<0739:catoc>2.3.co;2.
- Manabe, S., and R. Wetherald, 1967: Thermal equilibrium of the Atmosphere with a given Distribution of Relative Humidity. *Journal of Atmospheric Science*, 24, 241-258.

Mauritsen, T., and B. Stevens, 2015: Missing iris effect as a possible cause of muted hydrological change and high climate sensitivity in models. *Nature Geoscience*, 8, 346-351, doi:10.1038/ngeo2414.

May, P., and D. Rajopadhyaya, 1999: Vertical Velocity Characteristics of Deep Convection over Darwin, Australia. *Monthly Weather Review*, 127, 1056-1071, doi:10.1175/1520-0493(1999)127<1056:vvcodc>2.0.co;2.

Met Office, 2018: Stratocumulus clouds, Accessed July 25, 2018.

<https://www.metoffice.gov.uk/learning/clouds/low-level-clouds/stratocumulus>

Muller, C.: Caroline Muller Home Page. *Off-ladhyx.polytechnique.fr*,. Accessed July 25, 2018, <http://www.off-ladhyx.polytechnique.fr/people/muller/> .

NASA, 2009: Climate and Earth's Energy Budget. *Earthobservatory.nasa.gov*,. Accessed July 25, 2018. <https://earthobservatory.nasa.gov/Features/EnergyBalance/page5.php>

Neggers, R., P. Duynkerke, and S. Rodts, 2003: Shallow cumulus convection: A validation of large-eddy simulation against aircraft and Landsat observations. *Quarterly Journal of the Royal Meteorological Society*, 129, 2671-2696, doi:10.1256/qj.02.93.

Pauluis, O., and S. Garner, 2006: Sensitivity of Radiative–Convective Equilibrium Simulations to Horizontal Resolution. *Journal of the Atmospheric Sciences*, 63, 1910-1923, doi:10.1175/jas3705.1.

Plank, V. G., 1969: The size distribution of cumulus clouds in representative Florida populations. *Journal of Applied Meteorology*, 8, 46-67.

Pruppacher, H.R., Klett, J.D., 1997. *Microphysics of Clouds and Precipitation*, 2nd Edn. Kluwer Academic Publishers, Boston.

Riehl, H., and J. S. Malkus (1958), On the heat balance in the equatorial trough zone, *Geophysica*, 6, 503– 538.

Rochetin, N., B. Lintner, K. Findell, A. Sobel, and P. Gentine, 2014: Radiative–Convective Equilibrium over a Land Surface. *Journal of Climate*, 27, 8611-8629, doi:10.1175/jcli-d-13-00654.1.

Scheufele, K., 2014: Resolution dependence of cumulus statistics in radiative-convective equilibrium. University of Munich.

Siebesma A.P. (1998) Shallow Cumulus Convection. In: Plate E.J., Fedorovich E.E., Viegas D.X., Wyngaard J.C. (eds) *Buoyant Convection in Geophysical Flows*. NATO ASI Series (Series C: Mathematical and Physical Sciences), *Springer*, Dordrecht, 513, 441-486, doi:10.1007/978-94-011-5058-3_19.

Stevens, B., 2005: Atmospheric moist convection. *Annual Review of Earth and Planetary Sciences*, 33, 605-643, doi:10.1146/annurev.earth.33.092203.122658.

Turner, A. (2018), MTMG 19, Tropical weather system, University of Reading.

University of Wyoming: Cloud liquid water content, drop sizes, and number of droplets. *Www-das.uwyo.edu*, Accessed July 28, 2018, http://www-das.uwyo.edu/~geerts/cwx/notes/chap08/moist_cloud.html

Wageningen university and research, 2010:*Met.wur.nl*,. Accessed July 25, 2018, <http://www.met.wur.nl/education/atmospract/unit13/convective%20clouds.pdf>

Wing, A., K. Emanuel, C. Holloway, and C. Muller, 2017: Convective Self-Aggregation in Numerical Simulations: A Review. *Surveys in Geophysics*, 38, 1173-1197, doi:10.1007/s10712-017-9408-4.

Yang, J., Z. Wang, A. Heymsfield, and J. French, 2016: Characteristics of Vertical Air Motion in Convective Clouds. *Atmospheric Chemistry and Physics Discussions*, 1-48, doi:10.5194/acp-2015-1021.

Robertes, N.: Met Office, *Research.ncl.ac.uk*,. Accessed July 25, 2018

https://research.ncl.ac.uk/media/sites/researchwebsites/convex/4_Royal_society_Roberts.pdf

Appendix A – Abstract

‘Evolution of Science: Past, Present and Future Conference’

5th – 6th July 2018

University of York, UK

Organized by Royal Meteorological Society

Moist convection plays major role in the energy balance on Earth by transporting moist static energy to upper troposphere, by interacting with the global circulation and by mass exchange between troposphere and stratosphere. Also, deep convection clouds can produce high intensity rainfalls which can initiate flash floods. Therefore, convection forecasting gains lot of attention. Many “convection permitting” numerical models run in the range of 1-4 km resolution which simulate convective clouds explicitly without the need for a parameterization. Even though these models have many benefits, the grid spacings are not good enough to capture all cloud properties such as size, shape, rain rate etc since convection is a localized phenomenon. In this study, clouds were simulated at finer resolutions to determine cloud property variation. The aim is to investigate which resolution and which physical mechanisms might determine cloud properties using the results produced by the new MONC (Met Office - NERC) cloud model, at resolutions ranging from 50 -3200 m. Cloud properties and distributions of cloud properties based on simulated clouds will be investigated to determine the best resolution which can be used with confidence.